Mosayebi-Samani, Mohsen; Agboada, Desmond; Mutanen, Tuomas P.; Haueisen, Jens; Kuo, Min Fang; Nitsche, Michael A.

Transferability of cathodal tDCS effects from the primary motor to the prefrontal cortex: A multimodal TMS-EEG study

Published in:
Brain Stimulation

DOI:
10.1016/j.brs.2023.02.010

Published: 01/03/2023

Document Version
Publisher's PDF, also known as Version of record

Brain Stimulation 16 (2023) 515–539

Contents lists available at ScienceDirect

Brain Stimulation

journal homepage: http://www.journals.elsevier.com/brain-stimulation

Transferability of cathodal tDCS effects from the primary motor to the prefrontal cortex: A multimodal TMS-EEG study

Mohsen Mosayebi-Samani [a, b], Desmond Agboada [a, c], Tuomas P. Mutanen [d], Jens Haueisen [b], Min-Fang Kuo [a], Michael A. Nitsche [a, e, *]

[a] Department of Psychology and Neurosciences, Leibniz Research Centre for Working Environment and Human Factors, Dortmund, Germany
[b] Institute of Biomedical Engineering and Informatics, Technische Universität Ilmenau, Ilmenau, Germany
[c] Institute of Psychology, Federal Armed Forces University Munich, Neubiberg, Germany
[d] Department of Neuroscience & Biomedical Engineering, Aalto University, School of Science, 00076, Aalto, Espoo, Finland
[e] Bielefeld University, University Hospital OWL, Protestant Hospital of Bethel Foundation, University Clinic of Psychiatry and Psychotherapy and University Clinic of Child and Adolescent Psychiatry and Psychotherapy, Bielefeld, Germany

ARTICLE INFO

Article history:
Received 18 July 2022
Received in revised form
24 January 2023
Accepted 19 February 2023
Available online 23 February 2023

ABSTRACT

Neurophysiological effects of transcranial direct current stimulation (tDCS) have been extensively studied over the primary motor cortex (M1). Much less is however known about its effects over non-motor areas, such as the prefrontal cortex (PFC), which is the neuronal foundation for many high-level cognitive functions and involved in neuropsychiatric disorders. In this study, we, therefore, explored the transferability of cathodal tDCS effects over M1 to the PFC. Eighteen healthy human participants (11 males and 8 females) were involved in eight randomized sessions per participant, in which four cathodal tDCS dosages, low, medium, and high, as well as sham stimulation, were applied over the left M1 and left PFC. After-effects of tDCS were evaluated via transcranial magnetic stimulation (TMS)-electroencephalography (EEG), and TMS-elicited motor evoked potentials (MEP), for the outcome parameters TMS-evoked potentials (TEP), TMS-evoked oscillations, and MEP amplitude alterations. TEPs were studied both at the regional and global scalp levels. The results indicate a regional dosage-dependent nonlinear neurophysiological effect of M1 tDCS, which is not one-to-one transferable to PFC tDCS. Low and high dosages of M1 tDCS reduced early positive TEP peaks (P30, P60), and MEP amplitudes, while an enhancement was observed for medium dosage M1 tDCS (P30). In contrast, prefrontal low, medium and high dosage tDCS uniformly reduced the early positive TEP peak amplitudes. Furthermore, for both cortical areas, regional tDCS-induced modulatory effects were not observed for late TEP peaks, nor TMS-evoked oscillations. However, at the global scalp level, widespread effects of tDCS were observed for both, TMS-evoked potentials and oscillations. This study provides the first direct physiological comparison of tDCS effects applied over different brain areas and therefore delivers crucial information for future tDCS applications.

1. Introduction

Application of weak direct current via electrodes placed over the scalp (transcranial direct current stimulation, tDCS) has been shown to alter cortical excitability over the primary motor cortex (M1) during, but also after the end of the intervention, inducing plasticity-like after-effects. The direction, magnitude, and duration of respective effects depend on stimulation parameters such as polarity and intensity/duration. Here, anodal tDCS, which refers to surface inward current over the target area, within certain dosage limits, typically results in enhancement of motor cortical excitability, however cathodal tDCS, which refers to outward current over the target area, reduces it [1–3]. This thus opens a window to shed light on brain functions underlying cognitive functions [4] or alter symptoms of neurological and psychiatric disorders accompanied by pathological alterations of cortical excitability [5].

* Corresponding author.Department of Psychology and Neurosciences, Leibniz Research Centre for Working Environment and Human Factors, Dortmund, Germany
E-mail address: nitsche@ifado.de (M.A. Nitsche).

https://doi.org/10.1016/j.brs.2023.02.010

The neurophysiological effects of tDCS over the M1 were largely taken as a template so far for the use of this intervention over non-motor regions, however previous findings show only gradual comparability between the M1 and other cortical areas. Over the sensorimotor cortex, anodal tDCS increased the amplitude of somatosensory potentials, however cathodal tDCS had no effects in one study [6], while another study showed excitability-diminishing effects of only cathodal tDCS [7]. Over the visual cortex, anodal tDCS enhanced, and cathodal tDCS reduced visual evoked potential amplitudes, however, the duration of the effects was relevantly shorter as compared to M1 stimulation with otherwise identical protocols [8]. Taking anatomical, as well as receptor and neurotransmitter distribution differences of distinct cortical areas into account, these gradual differences of effects are plausible and require direct physiological tests of tDCS over respective target areas [4].

This is of critical importance, as in addition to the tDCS applications in basic research and clinical settings of the motor domain, its effects have been also extensively explored for the treatment of neuropsychiatric diseases [9], and exploration of physiological mechanisms underlying cognitive functions, with the dorsolateral prefrontal cortex (DLPFC) as target region [10–12]. However, the neurophysiological effects of tDCS over this area have been much less explored. Application of concurrent transcranial magnetic stimulation (TMS) and electroencephalography (EEG), opened up a window to address the effects of tDCS on cortical excitability of different brain regions, as indexed by TMS-evoked potentials (TEPs) recorded from scalp EEG electrodes [13].

Few studies have employed TMS-EEG so far to evaluate tDCS effects. ***Over the M1***, anodal enhancement and cathodal inhibition of early TEP amplitudes have been observed for tDCS with 1 mA for 13 min [14], and 2 mA for 10 min [15]. ***For the prefrontal cortex (PFC)***, anodal tDCS with 1 mA for 20 min, applied with bipolar and high-definition tDCS (HD-tDCS), induced likewise an increase of local early TEP peaks, and a decrease of TMS-evoked beta and gamma oscillatory power over posterior EEG channels [16,17]. Another study, with a newly developed electrode configuration, tDCS with 1.5 mA for 14 min, targeting the left DLPFC with the anode, and the right DLPFC with the cathode, however, showed a reduction of late TEPs (about 120 ms after the TMS pulse) over only the parietal cortex, accompanied by a reduction of TMS-evoked power of theta and gamma oscillations at the global scalp level, whereas tDCS with opposite electrode positions had no effects [18]. Thus, most TMS-EEG studies so far indicated qualitatively comparable results of tDCS over the M1 and PFC, however, the number of studies is limited, and results are partially heterogeneous. A systematic comparative investigation of the neurophysiological effects of tDCS over these different brain regions is therefore required.

In a previous study, we systematically explored the dosage-dependent impact of cathodal tDCS over the M1, with different stimulation intensities (1, 2, and 3 mA, electrodes size 35 cm2), and durations (15, 20, and 30 min), via TMS-elicited motor evoked potentials (MEPs). Low and high-intensity protocols resulted in MEP amplitude reductions, whereas an excitability enhancement was observed after medium-intensity tDCS [19]. A respective twin study with anodal tDCS, but an otherwise identical experimental design, showed a relatively uniform enhancement of motor cortical excitability following different anodal tDCS dosages [20].

In the present study, we aimed to explore the transferability of cathodal tDCS effects from M1 to the PFC. In eight randomized sessions, four cathodal tDCS dosages of low, medium, and high intensity, as well as sham stimulation were applied over the left M1, and left PFC in all participants, with current densities at the scalp-electrode-interface identical to our previous motor cortex MEP study [19]. tDCS after-effects were then evaluated using TMS-EEG, and TMS-MEP approaches at the regional and global scalp level for TEP and MEP amplitude changes, and TMS-evoked oscillations. In line with recent findings, we further assessed the association between cortical and corticospinal excitability alterations [15], as well as tDCS-induced electrical fields (EFs) [21,22]. In the present study, we focused on cathodal tDCS effects, and explored the transferability of their non-linear dosage-dependency from M1 to the PFC. Although the majority of tDCS studies was conducted with anodal tDCS so far, excitability-diminishing effects of cathodal tDCS have gained increased interest recently, including clinical applications for cortical excitability reductions of epileptogenic tissue [23,24] and other neurological disorders [25,26]. Especially here, knowledge about the transferability of tDCS effects between areas and dosages is critical because of the non-linear dosage-dependent effects of cathodal tDCS, as shown in the motor cortex. Since the addition of anodal tDCS to this study would have resulted in an excessive number of sessions, respective data will be obtained in a parallel study.

Based on previous findings, we anticipated dosage-dependent nonlinear MEP amplitude modulations for motor cortex tDCS, with low and high dosages diminishing MEP amplitudes, but an enhancement of MEP amplitudes via medium dosage tDCS, as compared to the respective baseline and/or sham conditions. In previous studies, 1 mA and 3 mA cathodal M1-tDCS for 20min reduced MEPs, while 2 mA cathodal tDCS for 20min resulted in an MEP amplitude enhancement [19,27]. This could be explained by the calcium-dependency of the directionality of tDCS effects on cortical excitability, as shown by previous studies [28–30]. Indeed, the strength and directionality of the effects of a tDCS protocol depend on the specific level of NMDA receptor, andcalcium channel activation, leading to corresponding amounts of Ca^{2+} influx. In this line, the switch from LTD- (induced by 1 mA cathodal tDCS) to LTP-like plasticity (induced by 2 mA cathodal tDCS), is assumed to be due to an enhancement of Ca^{2+} influx to a level sufficient for induction of LTP-like plasticity. Further enhancement of Ca^{2+}influx via intensified protocols (here 3 mA cathodal tDCS) will then activate counter-regulatory mechanisms due to calcium overflow, which would cause LTD-like plasticity due to activation of hyperpolarizing potassium channels, which will again reduce calcium influx [31]. We expected similar effects on early TEPs, according to preliminary evidence suggesting close associations between these two measures of cortical excitability [32–35], but could not rule out gradual differences of tDCS effects on MEPs and TEPs, since the neural foundations of TEPs are only rudimentary understood. In addition, we expected similar effects with prefrontal stimulation, because of similar stimulation dosage at the scalp level, but could not rule out gradually different patterns of neurophysiological effects of tDCS over the PFC, as compared to M1 tDCS, due to physical differences, e.g. differences of inter-electrode stimulation distance, and electrode to cortex distance, which result in different E-field induction at the respective cortical areas [21,36–40], neurophysiological differences [41], as well as differences of neurotransmitter concentration, and receptor distribution across cortical areas [42].

2. Material and methods

2.1. Participants

Since this is the first study investigating the transferability of tDCS-generated cortical excitability alterations from motor to prefrontal cortices, a literature-based, *a priori* sample size estimation could not be executed. Thus, a post hoc power calculation was performed using G*Power 3.1 [43]. The analysis was based on a repeated measures ANOVA with a medium to large effect size

$f = 0.35$ (corresponding to the average empirically obtained effect size $\eta_p^2 = 0.11$, see Table 3 and Table S2), $\alpha = 0.05$, and a sample size of 18 participants (11 males and 7 females, mean age 26.61 ± 3.56 years). This sample size resulted in a power of 0.96 and should mitigate the expected TEP variability across participants [44,45]. All participants were young, healthy, and right-handed according to the Edinburgh handedness inventory [46] and had no history of neurological and psychiatric diseases, or fulfilled exclusion criteria for noninvasive electrical or magnetic brain stimulation [47,48]. The study conformed to the Declaration of Helsinki and was approved by the local Ethics Committee of the Leibniz Research Centre for Working Environment and Human Factors. All participants gave written informed consent before starting the study and were financially compensated for participation.

2.2. Navigated TMS-EEG and -MEP measures

2.2.1. Transcranial magnetic stimulation

Single-biphasic TMS pulses were applied at 0.33 Hz (±30% jitter; which results in random inter-stimulus intervals between 2.1s and 4.0 s. The jitter was introduced to minimize expectancy effects, which could prominently affect TEP and MEP amplitudes) delivered by a PowerMag magnetic stimulator (Mag&More, Munich, Germany) with a figure-of-eight coil (PMD70) held tangentially over the EEG cap, with the handle pointing backwards and laterally at 45° from the midline.

For the M1 stimulation site, TMS pulses were first applied to determine the representational area of the right abductor digiti minimi (ADM) muscle, in which the largest MEPs were produced by a given medium TMS intensity. At this stimulation site, the resting motor threshold (RMT) was then determined by the TMS-Motor-Threshold-Assessment Tool (MTAT 2.0) [50–52]. Briefly, MTAT 2.0 estimates the RMT with a maximum likelihood parametric estimation by a sequential testing algorithm [53], which requires much less than the number of pulses needed for the conventional approach [52,54,55]. For the PFC stimulation site, in accordance with other studies in the field, the TMS coil was placed over the F3 position (10-10 international EEG standard), with the handle pointing backwards and laterally at 45° from the midline [16,56–58]. The F3 positioning was selected to approximate the scalp location overlaying the left DLPFC, in accordance with previous studies [16,59,60]. Note that, at the first experimental session of each participant, the identified TMS stimulation targets were stored in the navigation system, to be used throughout the experiment (see also section 2.3. Experimental procedures for details).

At each stimulation site, and for each time point, 120 single TMS pulses were applied with a stimulation intensity of 100% RMT. RMT was obtained for the M1 stimulation site with the TMS coil placed at about 5 mm distance to the surface of the head, due to the thin layer of Ten-20 paste, the tDCS electrode and the EEG cap between the coil and the skin. For the PFC stimulation site, we first measured RMT over the M1, with the TMS coil attached to the EEG cap and with a 4 mm thick foam in between, to keep the coil-to-head distance similar to that of the PFC stimulation site with a coil-to-head distance of about 5 mm because of the Ten-20 paste, the tDCS electrode and the EEG cap between the coil and the skin. The foam was then removed and the TMS coil was placed over the PFC stimulation target (F3). TMS intensity was 100% of RMT, to obtain reasonable effects of TMS on EEG responses [61], but minimize non-direct/unwanted effects of TMS, such as TMS-related artifacts [62] (decay and muscles artifacts; see section 2.4.1. 'TEP pre-processing'), and the TMS-induced clicking sound and coil vibration, which result in contamination of the EEG response with sensory and somatosensory responses [63,64].

2.2.2. EEG recording

A TMS-compatible EEG system (NeurOne, BittiumCorporation, Finland) was used to continuously record TEPs (DC-1.25 kHz) with a sampling frequency of 5 kHz. EEG signals were captured by TMS-compatible Ag/AgCl C-ring electrodes via a 64 electrode EEG cap (EasyCap, Herrsching, Germany). Electrodes were positioned according to the 10-10 international EEG standard. For both tDCS stimulation sites, eight EEG electrodes were excluded from data analysis due to the placement of the tDCS electrodes, including: C1, C3, C5, FC3, CP3, Fp2, AF4, and AF8 (for tDCS over M1), and F1, F3, F5, FC3, AF3, Fp2, AF4, and AF8 (for stimulation over the PFC)). Electrodes were online referenced and grounded to external electrodes placed on the forehead (above the nasion) [65,66]. Two additional electrodes were used to record horizontal and vertical eye movements (one on the orbital ridge centered directly below the left eye and the other one at the lateral junction of the upper and lower right eyelids) [65,66]. Impedances of all electrodes were kept below 5 kΩ during the experiment.

2.2.3. Navigated TMS

Following individual TMS stimulation site identification (see section 2.2.1), an MR-based 3D-navigation system (PowerMAG View, Mag&More, Munich, Germany) was employed to store and display online the position and orientation of the TMS coil with respect to the participant's head and fiducials based on an individual structural MRI scan, assuring accuracy and reproducibility of the stimulation outcome throughout the experiment [13]. All imaging data were acquired by a 3T Philips Achieva scanner (Best, Netherlands) with a 32-channel head coil. Anatomical images were recorded based on T1-weighted fast 3D gradient echo pulse sequences (repetition-time = 8179 ms, echo-time = 3.7 ms, flip-angle = 8°, 220 slices, matrix-size = 240x240, and resolution = 1x1x1 mm^3).

2.2.4. MEP recording

Surface EMG was recorded from the right ADM in a belly-tendon montage. The signals were amplified (Gain: 1000), band-pass filtered (2 Hz-2 kHz) using D440-2 (Digitimer, WelwynGardenCity, UK), and digitized (sampling rate: 5 kHz) with a micro 1401 AD converter (CED, Cambridge, UK), controlled by Signal Software CED, v.2.13.

2.2.5. Transcranial direct current stimulation

tDCS was applied with a constant-current battery-powered stimulator (neuroCare, Ilmenau, Germany), through a pair of surface rubber electrodes (25 cm2) attached on the scalp using conductive paste (*Ten20®, Weaver*). For the M1 stimulation sessions, the target electrode was centered over C3 and rotated 45° towards the midline. For the PFC stimulation sessions, the target electrode was centered over the F3 position, parallel to the midline. The return electrode, for both stimulation sites, was located over the contralateral supraorbital region. In the first session, the individual distance between the center of the target tDCS electrode and Cz and CPz (for M1-stimulation sessions) or AFz and FCz (for PFC-stimulation sessions), and F4 to the center of the return electrode (for both stimulation sites), were measured, and individual photographs of tDCS electrode positions were taken. These positions were then used for all following tDCS sessions. This improved tDCS electrode positioning consistency across sessions. Prior to electrode placement, a topical anesthetic cream (*EMLA®, AstraZeneca, UK*) was applied to the respective stimulation sites, in order to decrease somatosensory sensations and sufficiently blind the participants [67]. In eight randomized sessions, four cathodal tDCS dosages of low (0.7 mA for 15 min), medium (1.4 mA for 20 min), and high (2.1 mA for 20 min) intensities, and sham (for 15 min), were applied

over the two stimulation sites M1 and PFC. We chose stimulation parameters (intensity and duration) based on the results of our former MEP study suited to cover the bandwidth of magnitude, and direction of effects [19], but used smaller stimulation electrodes (25 cm2 instead of 35 cm2) to sacrifice fewer EEG channels around the tDCS target sites. Therefore, the same current densities at the scalp-electrode interface as in the previous study were applied for low (0.028 mA/cm2), medium (0.057 mA/cm2), and high (0.085 mA/cm2) dosages of tDCS. For sham stimulation, 0.7 mA stimulation was delivered for 15 s followed by 15 min with 0.0 mA stimulation.

All protocols were conducted with a 10 s ramp-up and -down at the start, and end of stimulation. The tDCS sessions were applied in randomized order with a minimum of seven days between sessions to avoid carry-over effects [68].

2.3. Experimental procedures

The study was performed in a cross-over single-blinded sham-controlled repeated measures design (Fig. 1). At the beginning of each session, participants were seated in a comfortable chair with head- and arm-rests. Afterwards, the topical anesthetic cream was applied over the scalp at the identified corresponding tDCS stimulation sites, and the tDCS electrodes were attached to the head with conductive paste (note that, to improve the consistency of tDCS electrode positing across sessions, the positions identified in the first session were used throughout the experiments; see section 2.2.5 for details), followed by the set-up of the EEG cap. The participant's head was then co-registered to the individual head model within the navigation system. Thereafter, the TMS coil was placed over the identified/stored positions in the first session (for the M1 stimulation site (representational area of the right ADM muscle) and PFC stimulation site (the F3 position (10-10 international EEG standard)); see section 2.2.1 for details). Subsequently, TMS intensity was adjusted to the RMT (as explained above). Then baseline cortical excitability was determined by TMS-EEG over M1 (including also simultaneous MEP recording) or PFC stimulation sites, depending on the tDCS stimulation session. Afterwards, the respective tDCS protocol was applied. Finally, cortical excitability was monitored by TMS-EEG immediately (POST0), 30 min (POST30), 60 min (POST60), and 120 min (POST120) after tDCS, Fig. 1. Concurrent with TEP recording, the participants were exposed to white noise through headphones to minimize contamination of the EEG signal by auditory evoked potentials, induced by the TMS-related clicking sound [64,69,70]. Here, prior to the start of the main experiment, the loudness of the 'noise masking' sound was systematically measured (using Sound level

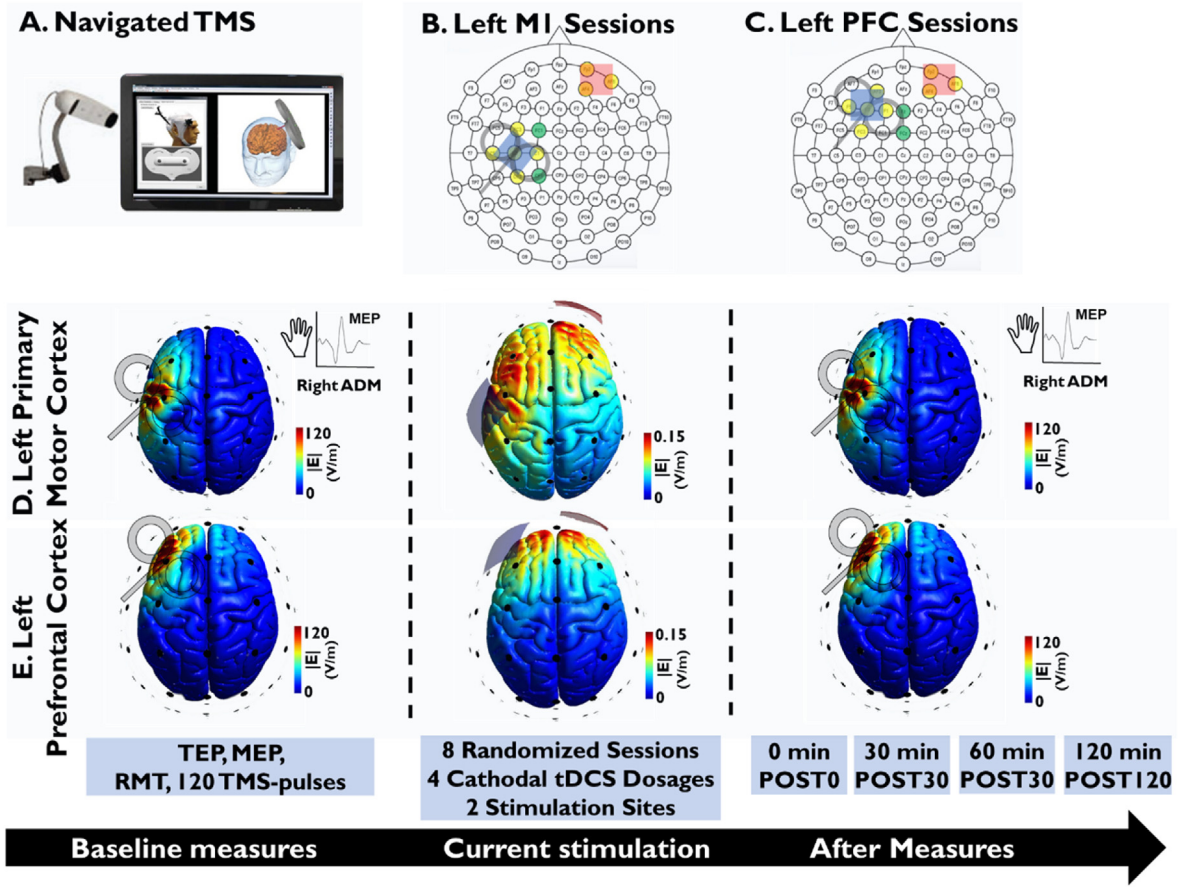

Fig. 1. Course of the study. In eight randomized sessions, four cathodal tDCS dosages of low (0.028 mA/cm^2; 15 min), medium (0.057 mA/cm^2; 20 min), and high (0.085 mA/cm^2; 20 min) intensity, as well as sham stimulation (0 mA; 15min) were applied to target the left primary motor (left M1; **B, D**), and left prefrontal cortex (left PFC; **C, E**). To evaluate the modulatory effects of tDCS, using a navigated TMS system (**A**), TMS-evoked cortical reactivity, and TMS-elicited MEP (only for tDCS applied over the M1), were recorded before tDCS, and immediately (POST0), 30 min (POST30), 60 min (POST60), and 120 min (POST120) after tDCS, with 120 TMS pulses at each time-point. The recorded data were then evaluated for TMS-evoked potentials (TEPs), oscillations, and MEP alterations. **B and C** show the pictogram of the tDCS electrode montage for the 10-10 EEG system, with 1) the target tDCS electrode (blue), 2) the return electrode (red), 3) the EEG electrodes that were removed due to the placement of tDCS electrodes (yellow), 4) selected ROIs over each stimulation site (green), and 5) the TMS coil over the targeted area. Colors in the cortical grey matter are illustrating electric field magnitudes induced by TMS and tDCS (0.7 mA) estimated via SimNIBS open-source software with its default parameters and head model (MNI.msh) [49]. (For interpretation of the references to color in this figure legend, the reader is referred to the Web version of this article.)

Analyzer B&K 2250, Brüel & Kjær, Denmark) and respective values were then used for controlling the upper safety threshold (95 db). During the experiment, the sound level was gradually increased until the participant could not hear the "click" sound of the TMS coil, or until it had reached the upper safety threshold [64,66].

2.4. Calculations

Offline data processing was performed with custom scripts in MATLAB (R2019b, Mathworks, USA), Fieldtrip [71], Brainstorm [72], and FreeSurfer [73] toolboxes.

2.4.1. MEP and TEP preprocessing

MEP amplitudes were first visually inspected to exclude MEP trials: 1) in which background electromyographic activity was present, and 2) which were associated with respective bad TEP trials (see below). Then, the individual means of peak-to-peak MEP amplitudes, recorded at each time-point, were separately calculated for all subjects and all conditions.

TEP preprocessing: first, a time period (−5 to +15 ms) around each TMS pulse was removed and interpolated ('cubic spline function'). This time period was selected to effectively minimize the TMS-related artifacts with very large amplitudes (e.g., ringing, muscle, or decay; here lasting until ~15 ms from the onset of TMS, Fig S1)), thus improving the performance of the following preprocessing steps [74–77]. It has been shown that minimizing the amplitude of TMS-evoked muscle activity with independent component analysis (ICA) improves the recovery of the TMS-evoked potentials for the time period starting ~ 15 ms after the onset of the TMS pulse [75–77]. Then the EEG data were segmented into epochs around the TMS pulses (−1000–1500 ms), and visually inspected to remove bad trials/channels. This includes data containing very large artifacts (i.e. signals exceeding 100 μV), electromagnetic residuals, muscle activity signals (e.g. TMS-related or jaw-clenching muscle activity), or other abnormal activity [74,76,78–80]. Then the EEG data were referenced to the average of all electrodes. Afterwards, the data were high-pass filtered (1Hz; 4th-order zero-phase Butterworth) and preprocessed with the 'signal-space projection with source-informed reconstruction' (SSP-SIR) algorithm. SSP-SIR is a spatial filtering method, which has been shown to efficiently suppress TMS-related muscle artifacts [62,81]. For that, we formed subject-specific, realistic lead field matrices, by first automatically segmenting the individual T1-weighted MRI images using Freesurfer software [73], which were then imported to Brainstorm toolboxes [72], to generate lead fields, based on the three-layer symmetric boundary element method via OpenMEEG [82] (tissue conductivity values (S/m): scalp = 0.33, skull = 0.0033, and brain = 0.33; standard 10-10 EEG electrode location adapted by MR-based participant's fiducials). Then, SSP-SIR was applied to project out artifacts during the first 50 ms after the TMS pulse. We identified the principal components (based on principal component analysis; PCA) that explained more than 90% of the variance of the high-pass filtered data (above 100Hz) in the EEG trials and removed those from the TEP data (on average: 6.8 ± 1.3) [81]. The SSP-SIR algorithm first applies a 100Hz high-pass filter to the input data to estimate the relative-amplitude kernel of the artifact and use this to project out the artifacts (here muscle artifacts) from the original input data. Data were then low-pass filtered (100Hz; 4th-order zero-phase Butterworth) following an independent component analysis (FastICA) to manually remove remaining noise components, including exponential decay, blinking and eye movements, muscle artifacts, line noise, and other noise-related artifacts, by looking at the time-course, spectral signature and topographical representation of the components [74,77,79,83,84]. Prior to the ICA, the rank of input data was checked to ensure that the number of the searched components (N = 30) was never bigger than the rank of the data matrix [76]. Finally, the decomposed data were filtered (lowpass: 45 Hz; 4th-order, zero-phase Butterworth), baseline-corrected (baseline EEG was obtained from −1000 to −50 ms relative to TMS onset; a period not closer than −50 ms to the TMS pulse was chosen to avoid contamination from the TMS artifact [18]), and bad channels were interpolated (according to the distance from neighboring channels; note that only bad EEG channels were interpolated, but not the EEG channels that were removed due to the placement of tDCS electrodes; see section 2.2.2). Following pre-processing of TMS-EEG data, the trials were averaged for the TEP calculations (see section 2.4.2). Also, the TMS-evoked oscillations were calculated on a single trial basis and then averaged across trials (please see section 2.4.3). For the included number of trials, removed MEPs, and ICA components, please refer to supplementary materials Table S1. See also Fig S1, which includes a schematic pipeline and also two individual datasets, to aid researchers in dealing with TMS-EEG data and to show the efficacy of the preprocessing steps from the raw data to the processed TMS-evoked cortical reactivity across all EEG channels. See also Fig S2, which included individual averaged TMS-evoked potentials following sham measures, and Fig S3, which included grand-averaged TEPs across all subjects following sham, Low-, Medium-, and high-dosage tDCS over the left M1(Baseline and POST0 (immediately after the end of stimulation)) and left PFC (Baseline and POST0 (immediately after the end of stimulation)).

2.4.2. TMS-evoked potentials

To evaluate the regional effects of tDCS applied over M1, and the PFC, we averaged the TEP deflections measured by the FC1 and CP1 electrodes (region of interest (ROI_{M1}), and the FCz and Fz electrodes (ROI_{PFC}), respectively. These ROIs were selected to capture the regional effects of tDCS, as they are located close to the tDCS target electrode, are distant from cranial muscles, which are a source of TMS-related artifacts [16,62], and do not overlap between the two tDCS stimulation sites (M1 and PFC), Fig. 1.

For these ROIs, the known TEP peaks were first identified by searching the maximum (for positive) or minimum value (for negative deflections). TEP deflections were identified for the following time periods of 20–40 ms (P30), 35–55 ms (N45), 45–75 ms (P60), 85–135 ms (N100), and 170–230 ms (P200) [13,61,85,86]. A 10 ms window (±5 ms) around each identified TEP peak was then averaged to calculate the respective TEP amplitude, to be used for further statistical analysis [16].

In addition, respective analyses were also performed to explore global and widespread effects of tDCS in two dimensions: 1) the contalateral M1 and PFC stimulation sites, namely the right M1, and PFC, to explore tDCS effects on transcallosal activity [87,88] and 2) the global scalp level (see statistical methods (2.8.2.2) for details).

2.4.3. TMS-evoked oscillations

To test if tDCS modulated TMS-related neural oscillations, time-frequency representations (TFRs) of oscillatory power were calculated for ROI_{M1} and ROI_{PFC} on a single trial basis (Morlet wavelet; wavelet width: starting from 2.6 cycles and adding 0.2 cycle for each 1 Hz), and then normalized (db) to the respective baseline (−500 to −100 ms). Finally, frequency power estimates were calculated for four separate frequency bands (FBs), including Theta (θ; 4–7 Hz), Alpha (α; 8–13 Hz), Beta (β; 14–29 Hz) and Gamma (γ; 30–45 Hz) within the time window of 50–300 ms after the TMS pulse for all frequency bands [18].

In addition, respective analyses were also performed to explore global and widespread effects of tDCS in two dimensions: 1) the contalateral M1 and PFC stimulation sites, namely the right M1, and

PFC, to explore tDCS effects on transcallosal activity [87,88] and 2) the global scalp level (see statistical methods (2.8.2.4) for details).

2.4.4. Discriminability and qualitative assessment of tDCS protocols

After finishing each session, participants were asked to fill in a questionnaire which contained: 1. Guessed intensity of tDCS (none, low, medium, high) 2. Rating scales for evaluation of the presence and amount of visual phenomena, itching, tingling, and pain during stimulation, and 3. Rating scales for evaluation of the presence and amount of skin redness, headache, fatigue, concentration difficulties, nervousness, and sleep problems within 24 h after stimulation. The side-effects were rated on a numerical scale ranging from zero to five, zero representing no and five extremely strong sensations [89,90].

2.4.5. Computational modeling of tDCS- and TMS-induced electrical fields

Using the individual T1 image of each participant, the tDCS- and TMS-induced EFs were estimated with a free and open-source software package for the simulation of non-invasive brain stimulation (SimNIBS v.3.2.3) [49]. Briefly, this includes T1 image segmentation into the major head tissues, 3D volume reconstruction, placement of tDCS electrodes (for tDCS-induced EF estimation: C3-Fp2 for M1 stimulation and F3-Fp2 for tDCS over the PFC; electrode size 5*5 cm), or locating the TMS coil (figure-of-8 shape, 5 mm above the head to approximate the actual experimental condition; $\frac{dI}{dt} = 1\ A/\mu s$), assigning the respective tissue conductivities (white matter: 0.15 S/m, grey matter (GM): 0.4 S/m, CSF: 1.79 S/m, eyeballs, and scalp: 0.33 S/m, skull: 0.008 S/m), and calculating the tDCS- (for low (0.7 mA), medium (1.4 mA), and high-dosage (2.1 mA) intensity)- and TMS-induced EFs using the finite element method, under the quasi-static approximation [91]. Then, for each participant and each stimulation site (M1 and PFC), a mask was created over the GM, where the TMS-induced EF was $> \frac{\sqrt{2}}{2} EF_{max}$ (the half power region, which is a standard measure of the focality of TMS-induced EFs over the targeted area [92,93]). Finally, the tDCS-induced EFs (strength: |E|; 95% percentile) over the masks were calculated (Fig. 11C, Figure S8, Figure S9). Note that, due to the quasi-static approximation, the TMS-induced EFs can linearly be scaled to the other TMS intensities or corresponding dI/dt. Thus, we used normalized EF ($\frac{EF}{EF_{max}}$) values to create the respective individual mask over the GM, where ($\frac{EF}{EF_{max}} > \frac{\sqrt{2}}{2}$), which are identical across different stimulation intensities, for more details see Figure S10 or [21,94,95].

2.5. Statistics

All statistical analyses were performed using SPSS (IBM Corp. v.26.0), custom scripts in MATLAB, and the Fieldtrip toolbox [71]. The normality of data distribution was assessed with the Kolmogorov-Smirnov test. No significant deviations from normality were detected (for details see supplementary materials Table S1). Also, for all ANOVAs, Mauchly's test of sphericity was conducted, and the Greenhouse-Geisser correction was applied when necessary. The critical significance level was set at $p \leq 0.05$. Post hoc tests were conducted using the Fisher Least Significant Difference test in case of significant ANOVA results.

2.5.1. Baseline measures

At the regional level (ROI_{M1}, ROI_{PFC}), to test if baseline measures differed between sessions within and/or between stimulation sites, two-way repeated-measure ANOVAs (rmANOVA) were performed, with condition (4 levels) and stimulation site (2 levels) as within-subject factors, and baseline of TEP peak, or TFR of each frequency band, as dependent variables. In addition, for each stimulation site, a one-way rmsANOVA was performed, with condition (4 levels) as within-subject factors, and baseline of TEP peak, or TFR of each frequency band, as dependent variables. Furthermore, two separate one-way rmANOVAs were performed with condition (8 levels for TMS_{RMT}, 4 levels for baseline MEP) as within-subject factor, and TMS_{RMT} intensity, or baseline MEP as dependent variables, respectively.

Furthermore, at the global scalp level, to test if baseline measures were comparable between tDCS sessions within stimulation sites, cluster-based nonparametric permutation tests were used, based on the Monte-Carlo method [96], to effectively control for multiple comparisons across numerous EEG channels and time-points [96]. The clusters were defined as ≥2 neighboring electrodes with a p-value<0.05 (t-test), the number of permutations was 5000, and Monte-Carlo two-tailed p-values were defined for a critical α level of $p < 0.05$ [16,44]. For the TMS-evoked potentials we selected a time period of 20–250 ms after TMS and for TMS-evoked oscillatory data a time period of 50–300 ms for all frequency bands [18]. These time intervals were selected to avoid any a priori assumptions and also improve the methodological compatibility with the regional analysis. For the permutation tests within each stimulation site, we have excluded the missing EEG electrodes due to the placement of tDCS electrodes (8 electrodes for each stimulation site; see section '2.2.2. EEG Recording' for details). However, for comparisons between stimulation sites, this would result in a high total number of missing EEG electrodes (N = 13). We therefore conducted the global scalp analysis for each stimulation site separately, with otherwise identical parameters, except for the included channels. The same parameters were used for the further global scalp analysis.

2.5.2. Modulatory effects of tDCS and motor-to-prefrontal transferability

2.5.2.1. tDCS-altered TMS-evoked potentials (regional effects). We investigated if, at the regional level (ROI_{M1}, ROI_{PFC}), the tDCS-induced after-effects differed from respective sham conditions between active stimulation conditions within each stimulation site, and if effects of the tDCS protocols differed between the M1 and PFC stimulation sites. To this end, individual means of the TEP peaks after tDCS were first normalized (Δ) to the respective individual mean baseline: $(post.tDCS - baseline)/|baseline|$. Then, three-way rmANOVAs were calculated with condition (4 levels), time-point (4 levels; POST0, POST30, POST60, and POST120), and stimulation site (2 levels) as within-subject factors, and the normalized value of each TEP peak (ΔP30, ΔN45, ΔP60, ΔN100, ΔP200), as the dependent variable. Moreover, two-way confirmatory rmANOVAs, for each stimulation site separately, were calculated with condition (4 levels) and time-point (4 levels) as within-subject factors, and the normalized value of each TEP peak as the dependent variable. This has been done to ensure the consistency of the results obtained in respective 3-way ANOVAs, for each stimulation site separately.

In addition, we investigated within and between each stimulation site, if the tDCS after-effects differed vs. baseline values, using the absolute values. The respective analysis, and results (including figures and tables) can be found in the supplementary materials.

2.5.2.2. tDCS-altered TMS-evoked potentials (global scalp effects). We assessed the distributed effects of tDCS at two levels. First, we added the contralateral right hemispheric M1 and PFC to our analysis, to gain insight in tDCS effects on the contralateral homologue areas. For that, TEP deflections over the same time periods were extracted from 1) sets of right hemispheric control electrodes (for right motor cortex (ROI_{rM1}): C2, C4, C6, CP4; for the right

prefrontal cortex (ROI_{rPFC}): F2, F4, F6, FC4). These data were calculated the same way as in our principal analysis (rmANOVAs; see section 'TMS-evoked Potentials (regional effects')). Secondly, we performed a global scalp analysis of TMS-evoked potentials based on all available electrodes by cluster-based nonparametric permutation tests, based on the Monte-Carlo method [96]; see section '2.8.1. Baseline measures' for details of statistical parameters). We then investigated if within each stimulation site 1) the active intervention conditions altered cortical outcome measures versus baseline and 2) the after-effects of tDCS differed from the sham condition.

2.5.2.3. tDCS-altered TMS-evoked oscillations (regional effects). to assess the regional effects of tDCS on TMS-evoked oscillations, the same statistics (rmANOVAs; see section 'TMS-evoked Potentials (regional effects')) were performed, but here with TFRs of each FB (Theta, Alpha, Beta, and Gamma) as dependent variables.

2.5.2.4. tDCS-altered TMS-evoked oscillations (global scalp effects). To investigate the widespread and global effects of tDCS on TMS-evoked oscillations, the same statistics (see section 'TMS-evoked Potentials (global scalp effects') were performed, but here with TFRs of each frequency band (Theta, Alpha, Beta, and Gamma).

2.5.2.5. tDCS-altered TMS-elicited MEPs. we investigated if the tDCS after-effects on MEP amplitudes differed vs. sham, and between active stimulation conditions. To this end, two-way rmANOVAs were calculated with condition (4 levels; Low, Medium, High dosage, and Sham), and time point (4 levels; POST0, POST30, POST60, and POST120) as within-subject factors, and ΔMEP as the dependent variable. Another two-way rmANOVA were calculated with condition (4 levels), and time-point (5 levels; baseline, POST0, POST30, POST60, and POST120) as within-subject factors, and absolute values of the MEP measures as the dependent variable, to test if the tDCS after-effects on MEP amplitudes differed vs. baseline values.

2.5.2.6. Association between tDCS-generated TEP or MEP alterations, and tDCS-induced electrical fields. To explore associations between tDCS-generated TEP or MEP alterations, and tDCS-induced EFs, we calculated Pearson correlations for these variables. Furthermore, we explored the comparability of tDCS-induced EFs between the two stimulation sites via *Student's* paired t-tests. Due to the exploratory nature of these analyses, we did not correct for multiple comparisons.

2.5.3. Qualitative assessment of tDCS protocols

To identify if participants guessed tDCS intensities correctly, chi-square tests were conducted. Side-effects during and after tDCS were analyzed by a repeated measure ANOVA with condition (8 levels) as within-subject factor and rating scores (0–5) as the dependent variable. In case of significant effects, follow-up exploratory post-hoc paired t-tests were conducted to examine if an active session resulted in a significantly different sensation relative to sham.

3. Results

The distribution of the data was assessed with the Kolmogorov-Smirnov test and no significant deviations from normality were detected (for details see supplementary materials Table S1). For the respective preprocessing code and TMS-EEG datasets see https://cumulus.ifado.de/d/0e4669e8ca1c460d9a09/.

3.1. Baseline measures

The two-way rmANOVAs (condition '4 levels' and stimulation site '2 levels'), at the regional level, showed no significant differences in baseline TEP peaks within each stimulation site, however, significant differences between stimulation sites were observed for P30. Post-hoc tests indicated a lower amplitude of the P30 over the PFC, as compared to M1 (Table 1, Fig. 2 and Figure S4). Also, the respective rmANOVAs showed no significant differences for baseline TFRs of each frequency band within each stimulation site. However, significant differences were identified between stimulation sites for all frequency bands (except Theta), with lower power over the PFC, as compared to M1 (Table 1, Fig. 6, and Figure S6). Moreover, the one-way rmANOVAs (condition '4 levels'; performed for each stimulation site separately) showed no significant differences in baseline TEP peaks or TFRs of each frequency band within each stimulation site (Table 2). No significant differences were observed for either TMS_{RMT} (Table 1) or baseline MEP amplitudes between stimulation conditions (Table 1, Figure S7).

Also, at the global scalp level, using cluster-based permutation tests, no significant differences were observed between baseline measures of different tDCS dosages within each stimulation site.

3.2. Effects of tDCS and motor-to-prefrontal transferability

3.2.1. tDCS-altered TMS-evoked potentials (regional effects)

For the ΔP30 TEP, the three-way rmANOVA conducted with normalized values to compare the effects of each tDCS condition with sham, between active stimulation conditions within each stimulation site, and differences of tDCS effects between the M1 and PFC stimulation sites, showed significant main effects of condition and time-point, and a significant interaction of 'condition × time-point', but no main effect of stimulation site, or significances of other interactions (Table 3, Fig. 3). In the same vein, the confirmatory two-way rmANOVA (for each stimulation site separately; conducted with the normalized values), for M1 stimulation, resulted in significant main effects of 'condition' and 'time-point', but no significant effects of the respective interactions (Table 4). For the PFC stimulation site, the respective rmANOVA showed a significant main effect of 'condition' and a significant interaction of 'condition × time-point', but no significant main effects of 'time-point' (Table 4). Post-hoc tests comparing tDCS after-effects at the respective time points vs sham showed a significant ΔP30 amplitude reduction for low- (POST0) and high-dosage stimulation (POST0, POST30, POST60), while medium-dosage tDCS increased the TEP amplitude (POST0, POST30) for M1 tDCS. For PFC stimulation, the results showed a significant ΔP30 amplitude reduction for medium- and high-dosage (both at POST30 and POST60) tDCS, as compared to the respective sham condition (Fig. 3). In addition, post-hoc tests comparing active conditions within each stimulation site showed a larger ΔP30 amplitude for medium-dosage M1 tDCS (POST0,POST30,POST60), as compared to low- and high-dosage M1 tDCS (Fig. 3). Finally, post-hoc tests comparing conditions between stimulation sites indicated a significant difference for medium-dosage tDCS (POST30, POST60), with a larger P30 amplitude over the motor cortex, as compared to the prefrontal cortex (Table 3, Fig. 3). See supplementary materials for the results of the rmANOVA conducted with the absolute values (section S2.1; Figure S4, Table S2, and Table S3).

For the ΔN45 TEP, the three-way rmANOVAs (including also respective confirmatory analyses; conducted with normalized values) indicated no significant effects of tDCS protocols compared to sham values (Fig. 3, Table 3, Table 4). See supplementary materials for the results of the rmANOVA conducted with the absolute values (section S2.1; Figure S4, Table S2, and Table S3).

Table 1
Results of the ANOVAs conducted to evaluate baseline measurements. The ANOVAs (condition '4 levels' and stimulation site '2 levels') showed no significant differences of baseline measures within stimulation sites; however, significant differences were observed for the TEP P30 between stimulation sites, and FB for all frequency bands, except theta. Asterisks indicate significant effects ($p < 0.05$), d.f. = degrees of freedom, η_p^2 = partial eta squared, TEP = TMS-evoked Potentials and FB = frequency band.

Baseline Measures		Factors	d.f.	F value	p Value	η_p^2
TEPs	**P30**	**Condition**	3, 51	1.487	0.229	0.080
		Stimulation site	**1, 17**	**42.049**	**<0.001***	**0.712**
		Condition × Stimulation site	3, 51	0.576	0.633	0.033
	N45	**Condition**	3, 51	0.571	0.637	0.033
		Stimulation site	1, 17	0.001	0.973	0.001
		Condition × Stimulation site	3, 51	0.260	0.854	0.015
	P60	**Condition**	3, 42	1.658	0.191	0.106
		Stimulation site	1, 14	2.352	0.147	0.144
		Condition × Stimulation site	3, 42	0.375	0.771	0.026
	N100	**Condition**	3, 49	2.451	0.073	0.164
		Stimulation site	1, 15	0.201	0.660	0.013
		Condition × Stimulation site	3, 45	0.413	0.745	0.027
	P200	**Condition**	3, 51	2.367	0.526	0.156
		Stimulation site	1, 17	3.655	0.076	0.177
		Condition × Stimulation site	3, 51	1.382	0.259	0.075
TMS-evoked Oscillations	**Theta (θ)**	**Condition**	3, 51	1.930	0.137	0.102
		Stimulation site	1, 17	0.024	0.097	0.021
		Condition × Stimulation site	3, 51	1.58	0.198	0.101
	Alpha (α)	**Condition**	3, 45	1.109	0.355	0.069
		Stimulation site	**1, 15**	**27.927**	**<0.001***	**0.651**
		Condition × Stimulation site	3, 48	2.322	0.088	0.134
	Beta (β)	**Condition**	3, 51	1.569	0.208	0.084
		Stimulation site	**1, 16**	**88.042**	**<0.001***	**0.563**
		Condition × Stimulation site	3, 51	2.177	0.068	0.125
	Gamma (γ)	**Condition**	3, 27	0.125	0.356	0.111
		Stimulation site	**1, 9**	**72.140**	**<0.001***	**0.889**
		Condition × Stimulation site	3, 27	1.443	0.252	0.138
TMS_{RMT}		**Condition**	3.724, 63.315	1.466	0.079	0.226
MEP		**Condition**	3, 51	1.453	0.079	0.238

For the ΔP60 TEP, the three-way rmANOVA (including the factor stimulation site; conducted with the normalized values) resulted in a significant main effect of condition and a significant interaction of 'condition × time-point × stimulation site' ($F_{(4.648,55.777)} = 2.185$, $p = 0.035, \eta_p^2 = 0.122$), but no significant effects of the other main factors or interactions (Table 3, Fig. 3). In the same line, the confirmatory two-way rmANOVA (conducted for each stimulation site separately with the normalized values) for M1 stimulation resulted in significant main effects of 'condition' and time-point, but no significant effects of the respective interactions (Table 4). For the PFC stimulation site, the results of the two-way rmANOVA showed significant main effects of 'condition' and the 'condition × time-point' interaction, but no significant main effects of 'time-point' (Table 4). Post-hoc tests comparing tDCS after-effects to sham at the respective time points showed a significant ΔP60 amplitude reduction for low- and high-dosage stimulation over M1 (POST60). For PFC stimulation, the ΔP60 amplitude was significantly reduced vs sham for low- (POST0) and high-dosage tDCS (POST0 and POST30). In addition, post-hoc tests comparing active conditions within each stimulation site showed a larger ΔP60 amplitude for medium-dosage M1 tDCS (POST60), as compared to low- and high-dosage M1 tDCS; the same post-hoc tests conducted for tDCS over the PFC showed a larger ΔP60 amplitude for medium-dosage PFC tDCS (POST0), as compared to low- and high-dosage PFC tDCS (Fig. 3). See supplementary materials for the results of the rmANOVA conducted with the absolute values (section S2.1; Figure S4, Table S2, and Table S3).

For the ΔN100 and ΔP200 TEP, the respective three-way rmANOVAs (including also respective confirmatory analyses; conducted with normalized values) showed no significant effects of tDCS protocols, as compared to sham values (Tables 3 and 4, Fig. 3). See supplementary materials for the results of the rmANOVA conducted with the absolute values (section S2.1; Figure S4, Table S2, and Table S3).

In summary, the results showed non-linear dosage-dependent regional after-effects of tDCS over M1, as indicated by amplitude changes on early TEP peaks (P30 and P60) as compared to baseline, as well as compared to sham measures. However, a rather uniform reduction of early positive peaks was found for the tDCS after-effects over the PFC. No significant effects were however identified for the influence of tDCS on late TEP peaks in M1 or PFC tDCS conditions.

3.2.2. tDCS-altered TMS-evoked potentials (global scalp effects)

The three-way rmANOVAs (including stimulation site; conducted with the normalized values), conducted to assess if the after-effects of the active tDCS protocols on transcallosal TEPs differed vs. sham values showed no significant effect of neither the main factors condition, time-point, and stimulation sites, nor their respective interactions (Table S4). Moreover, the results of the confirmatory two-way rmANOVAs (conducted with the normalized values), conducted for M1 and PFC stimulation sites separately showed no significant main effects of 'condition' and 'time-point' or the respective interactions (Table S5). See also supplementary materials for the respective results of rmANOVAs conducted with the absolute values (section S2.2, Table S6, Table S7).

In addition, at the global scalp level, cluster-based permutation tests comparing the tDCS after-effects with respective baseline measures showed a negative cluster over the central electrodes (POST0; $p = 0.024$, time-period: 23–48 ms after TMS) and another negative cluster over the parieto-occipital electrodes (POST0; $p = 0.029$, time-period: 170–245 ms after TMS) for low-dosage ***tDCS over M1***). Likewise, a negative cluster was identified over the central electrodes (POST30; $p = 0.024$, time-period: 24–61 ms after TMS) and another negative cluster was revealed over the parieto-occipital electrodes (POST30; $p = 0.034$, time-period: 151–251 ms after TMS). For medium-dosage tDCS, a positive cluster was identified only over the central electrodes (POST30;

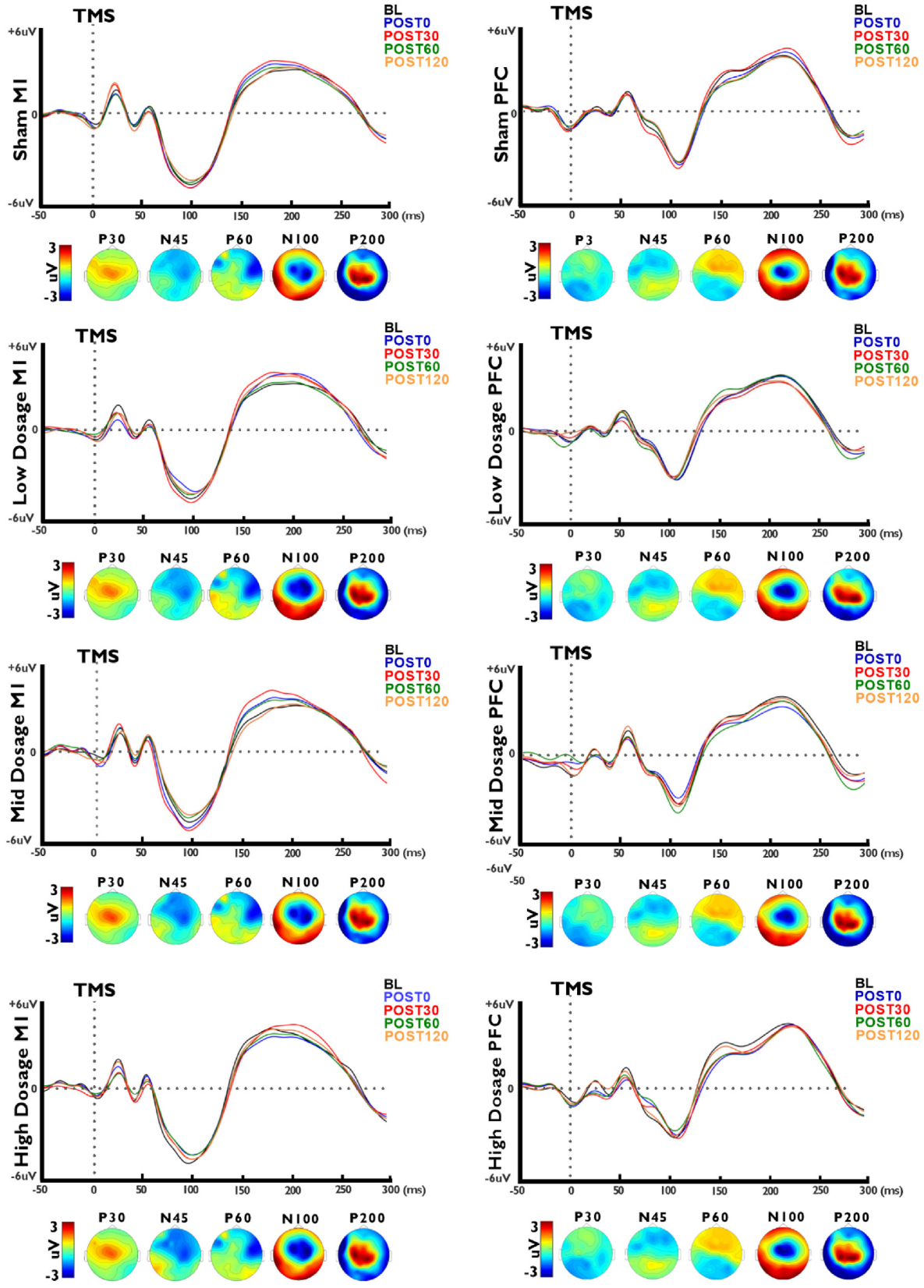

Fig. 2. Local effects of tDCS on TMS-evoked Potentials. Cathodal tDCS dosages of low, medium, and high intensities, and sham, were applied over the primary motor (M1) and left dorsolateral prefrontal cortex (PFC) stimulation sites. Local tDCS effects were obtained immediately (POST0) to up to 2 h after stimulation (POST30, POST60, POST120), over the ROI_{M1} (averaged FC1 and CP1 electrodes) and ROI_{PFC} (averaged FCz and Fz electrodes). Grand average across all subjects following tDCS conditions over the left primary motor cortex (ROI_{M1}; left column) and left DLPFC (ROI_{PFC}; right column), and topographic plots displaying voltage distributions across the scalp for each TEP peak ((P30, N45, P60, N100, P200) at the respective stimulation sites are shown.

Table 2
Results of the ANOVAs conducted to evaluate baseline measurements (conducted for each stimulation site separately). The one-way rmANOVAs (condition '4 levels'; performed for each stimulation site separately) showed no significant differences of baseline measures within each stimulation site. d.f. = degrees of freedom, η_p^2 = partial eta squared, TEP = TMS-evoked Potentials. M1: left motor cortex, PFC: prefrontal cortex. For all ANOVAs, Mauchly's test of sphericity was conducted, and the Greenhouse-Geisser correction was applied when necessary.

Baseline Measures		Factor/Stimulation-site	d.f.	F value	p value	η_p^2
TEPs	**P30**	**Condition/M1**	3, 51	0.709	0.551	0.040
		Condition/PFC	3, 51	1.471	0.233	0.080
	N45	**Condition/M1**	3, 51	0.184	0.907	0.011
		Condition/PFC	3, 51	1.309	0.283	0.072
	P60	**Condition/M1**	3, 51	0.733	0.537	0.044
		Condition/PFC	3, 51	1.129	0.348	0.070
	N100	**Condition/M1**	3, 51	2.208	0.098	0.115
		Condition/PFC	3, 51	0.192	0.901	0.011
	P200	**Condition/M1**	3, 51	2.114	0.110	0.111
		Condition/PFC	3, 51	0.279	0.840	0.016
TMS-evoked Oscillations	**Theta (θ)**	**Condition/M1**	3, 51	1.017	0.393	0.056
		Condition/PFC	1.766, 30.015	0.577	0.574	0.033
	Alpha (α)	**Condition/M1**	3, 51	0.276	0.842	0.016
		Condition/PFC	2.166, 36.830	0.456	0.653	0.026
	Beta (β)	**Condition/M1**	3, 51	0.727	0.541	0.041
		Condition/PFC	1.994, 33.897	2.684	0.082	0.178
	Gamma (γ)	**Condition/M1**	1.541, 28.017	1.522	0.250	0.145
		Condition/PFC	3, 51	0.241	0.868	0.014

p = 0.041, time-period: 21–54 ms after TMS). In addition, for high-dosage tDCS, a negative cluster was identified over the central electrodes (POST0; p = 0.028, time-period: 22–61 ms after TMS), over the parietal electrodes (POST0; p = 0.029, time-period: 70–148 ms after TMS), and another negative cluster was identified over the central electrodes (POST30; p = 0.024, time-period: 21–60 ms after TMS); Fig. 4. Moreover, the results of cluster-based permutation tests comparing the active tDCS conditions

Table 3
Results of the three-way ANOVAs conducted for tDCS-induced TEP alterations (conducted with the normalized values). The statistical results indicate tDCS-induced effects for the early (P30 and P60) TEP peaks, with no one-to-one transferability of tDCS effects from the motor to the prefrontal cortex. For all ANOVAs, Mauchly's test of sphericity was conducted, and the Greenhouse-Geisser correction was applied when necessary. See also Table S2 and Table S3 for the three- and two-way rmANOVAs conducted for tDCS-induced TMS-evoked potentials (conducted with the absolute values). Asterisks indicate significant effects ($p < 0.05$), d.f. = degrees of freedom, η_p^2 = partial eta squared.

	Factors	d.f., Error	F Value	p Value	η_p^2
ΔP30	**Condition**	**3, 30**	**9.610**	**<0.001***	**0.490**
	Time-point	**3, 30**	**3.382**	**0.031***	**0.253**
	Stimulation site	1, 10	0.568	0.469	0.054
	Condition × Time-point	**9.90**	**2.381**	**0.018***	**0.192**
	Condition × Stimulation site	1.378, 13.781	0.310	0.658	0.030
	Time-point × Stimulation site	3, 30	1.308	0.290	0.116
	Condition × Time-point × Stimulation site	9, 90	1.225	0.290	0.109
ΔN45	**Condition**	3, 15	0.294	0.829	0.056
	Time-point	1.262, 6.309	1.327	0.289	0.215
	Stimulation site	1, 5	2.444	0.179	0.328
	Condition × Time-point	9, 45	0.720	0.688	0.126
	Condition × Stimulation site	3, 15	1.372	0.289	0.215
	Time-point × Stimulation site	3, 15	1.055	0.398	0.174
	Condition × Time-point × Stimulation site	9, 45	1.626	0.137	0.245
ΔP60	**Condition**	**3, 15**	**3.441**	**0.034***	**0.408**
	Time-point	3, 20	1.054	0.405	0.174
	Stimulation site	1, 5	0.001	0.994	0.002
	Condition × Time-point	4.314, 51.763	0.431	0.799	0.035
	Condition × Stimulation site	3, 15	0.560	0.740	0.138
	Time-point × Stimulation site	4, 20	0.158	0.957	0.031
	Condition × Time-point × Stimulation site	**4.648, 55.777**	**2.185**	**0.035***	**0.122**
ΔN100	**Condition**	3, 42	2.518	0.071	0.152
	Time-point	3, 42	1.080	0.368	0.072
	Stimulation site	1, 14	0.611	0.447	0.042
	Condition × Time-point	9, 126	1.863	0.063	0.117
	Condition × Stimulation site	3, 42	0.931	0.434	0.062
	Time-point × Stimulation site	1.935, 27.095	1.568	0.227	0.101
	Condition × Time-point × Stimulation site	9, 126	1.147	0.335	0.076
ΔP200	**Condition**	3, 36	0.191	0.902	0.016
	Time-point	3, 36	2.432	0.082	0.168
	Stimulation site	1, 12	0.245	0.629	0.020
	Condition × Time-point	9, 108	0.770	0.645	0.060
	Condition × Stimulation site	3, 36	1.615	0.203	0.119
	Time-point × Stimulation site	3, 36	2.114	0.116	0.150
	Condition × Time-point × Stimulation site	3.611, 43.336	1.293	0.249	0.097

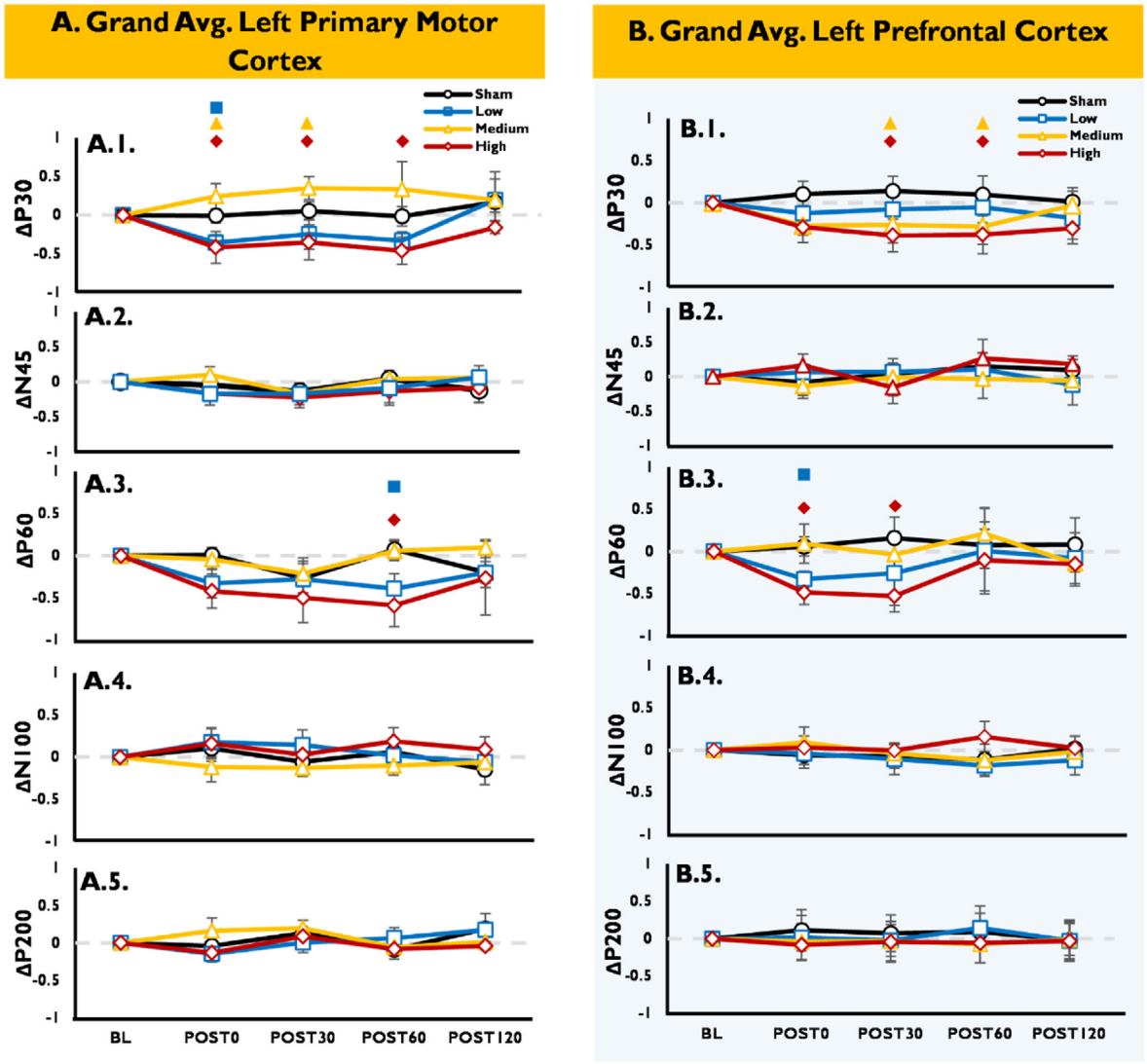

Fig. 3. Local effects of tDCS on TMS-evoked Potentials (normalized values). Low, medium, and high intensities of cathodal tDCS, and sham stimulation were applied over the primary motor (M1) and left dorsolateral prefrontal cortex (PFC). Local tDCS effects were then evaluated, every 30min, from immediately (POST0) to up to 2 h after stimulation (POST30, POST60, and POST120), over the ROI_{M1} (averaged FC1 and CP1 electrodes) and ROI_{PFC} (averaged FCz and Fz electrodes). A1-5, B1-5: normalized TMS-evoked potentials over M1 and the PFC, respectively. tDCS generated a dosage-dependent, partially non-linear modulation of TEP (ΔP30, ΔN45, ΔP60, ΔN100, ΔP200) over the different stimulation sites, as shown by the amplitude alterations of early ((ΔP30and ΔP60) TEP peaks. Floating symbols show a significant difference in active tDCS conditions (low-dosage ■, medium-dosage ▲, and high-dosage ◆) vs. sham. See Figure S4 for the local effects of tDCS on TMS-evoked Potentials (absolute values).

with sham measures showed a positive cluster for medium-dosage tDCS over M1 over the central electrodes (POST30; $p = 0.041$, time-period: 30–47 ms after TMS), a negative cluster for high-dosage tDCS over M1 over the centro-medial electrodes (POST0; $p = 0.032$, time-period: 24–65 ms after TMS) and another negative cluster over the centro-medial electrodes (POST30; $p = 0.021$, time-period: 31–86 ms after TMS), Figure S5.A-C.

For the distributed effects of ***tDCS over the PFC***, the cluster-based permutation tests comparing the tDCS after-effects with respective baseline measures showed for medium-dosage tDCS a negative cluster over the fronto-central electrodes (POST0; $p = 0.024$, time-period: 27–69 ms after TMS), a negative cluster over the fronto-central electrodes (POST30; $p = 0.036$, time-period: 62–87 ms after TMS) and another negative cluster over the central electrodes (POST30; $p = 0.034$, time-period: 79–111 ms after TMS). In addition, for high-dosage tDCS, a negative cluster was identified over the fronto-central electrodes (POST0; $p = 0.039$, time-period: 27–72 ms after TMS) and over central electrodes (POST30; $p = 0.024$, time-period: 21–60 ms after TMS), whereas a positive cluster was identified over a different group of central electrodes (POST30; $p = 0.026$, time-period: 148–253 ms after TMS); Fig. 5. Moreover, the results of the cluster-based permutation tests comparing the active tDCS conditions with sham measures showed a negative cluster for medium-dosage tDCS over the fronto-central electrodes (POST30; $p = 0.038$, time-period: 23–69 ms after TMS); a negative cluster for high-dosage tDCS over the centro-medial electrodes (POST0; $p = 0.042$, time-period: 34–86 ms after TMS) and another negative cluster over the right frontal electrodes for high-dosage tDCS (POST30; $p = 0.035$, time-period: 25–96 ms after TMS); Figure S5.D-F.

Together, these results indicate widespread effects of tDCS on TMS-evoked cortical reactivity at the global scalp level, which hints at the contribution of distant cortical networks on the overall tDCS efficacy.

3.2.3. tDCS-altered TMS-evoked oscillations (regional effects)

The three-way rmANOVAs (including the stimulation site; conducted with the normalized values), conducted to assess if the

Table 4
Results of the confirmatory two-way ANOVAs conducted for tDCS-induced TEP alterations (normalized values). The results of the confirmatory two-way ANOVAs (for each stimulation site separately; conducted with the normalized values) indicate tDCS-induced effects for the early (P30 and P60) TEP peaks at each stimulation site. For all ANOVAs, Mauchly's test of sphericity was conducted, and the Greenhouse-Geisser correction was applied when necessary. Asterisks indicate significant effects ($p < 0.05$), d.f. = degrees of freedom, η_p^2 = partial eta squared.

	Stimulation Site	Factors	d.f.	F Value	p Value	η_p^2
ΔP30	**M1**	**Condition**	**3, 51**	**7.430**	**<0.001***	**0.304**
		Time-point	**2.281, 38.798**	**3.821**	**0.026***	**0.184**
		Condition × Time-point	2.770, 47.089	1.136	0.342	0.063
	PFC	**Condition**	**3, 51**	**5.483**	**0.004***	**0.352**
		Time-point	3, 51	1.513	0.231	0.131
		Condition × Time-point	**9, 153**	**2.226**	**0.027***	**0.182**
ΔN45	**M1**	**Condition**	3, 51	0.750	0.530	0.059
		Time-point	3, 51	1.213	0.371	0.148
		Condition × Time-point	9, 153	1.553	0.139	0.115
	PFC	**Condition**	3, 51	0.363	0.780	0.039
		Time-point	1.043, 9.384	0.150	0.837	0.006
		Condition × Time-point	1.108, 9.974	0.062	0.833	0.007
ΔP60	**M1**	**Condition**	**3, 51**	**3.045**	**0.038***	**0.169**
		Time-point	3, 51	2.088	0.115	0.122
		Condition × Time-point	9, 153	1.341	0.222	0.082
	PFC	**Condition**	**3, 51**	**2.821**	**0.041***	**0.154**
		Time-point	3, 51	2.114	0.111	0.117
		Condition × Time-point	**9, 153**	**2.307**	**0.038***	**0.176**
ΔN100	**M1**	**Condition**	3, 51	0.752	0.453	0.063
		Time-point	3, 51	2.131	0.109	0.124
		Condition × Time-point	4.145, 62.174	1.341	0.264	0.082
	PFC	**Condition**	3, 51	0.684	0.566	0.041
		Time-point	1.937, 30.989	1.072	0.353	0.063
		Condition × Time-point	4.415, 70.643	1.773	0.138	0.100
ΔP200	**M1**	**Condition**	3, 51	0.693	0.562	0.055
		Time-point	3, 51	1.120	0.203	0.114
		Condition × Time-point	3.427, 41.130	1.187	0.311	0.090
	PFC	**Condition**	3, 51	1.157	0.336	0.067
		Time-point	3, 51	0.663	0.579	0.040
		Condition × Time-point	9, 153	0.852	0.570	0.051

after-effects of the active tDCS protocols on TMS-evoked oscillations differed vs. sham values, showed no significant effect of neither the main factors condition, time-point, and stimulation sites, nor their interactions (Table 5, Fig. 6, Fig. 7). In addition, the results of the confirmatory two-way rmANOVAs (for each stimulation site separately; conducted with the normalized values) conducted for M1 and PFC stimulation sites separately showed no significant main effects of 'condition' and 'time-point' or their respective interactions for all tested frequency bands (Table 6). See supplementary materials for the results of the rmANOVA conducted with the absolute values (section S2.3, Figure S6, Table S9, and Table S10).

3.2.4. tDCS-altered TMS-evoked oscillations (global scalp effects)

The three-way rmANOVAs (including stimulation site; conducted with the normalized values), conducted to assess if the after-effects of the active tDCS protocols on TMS-evoked oscillations of transcallosal activity differed vs. sham values, showed no significant effect of neither the main factors condition, time-point, and stimulation sites, nor their respective interactions (Table S11). Moreover, the results of the confirmatory two-way rmANOVAs (conducted with the normalized values), conducted for M1 or PFC stimulation sites separately, showed no significant main effects of 'condition' and 'time-point' or their interaction (Table S12). See also supplementary materials for the respective results of rmANOVAs conducted with the absolute values (section S2.4, Table S13, Table S14).

In addition, at the global scalp level, cluster-based permutation tests of TMS-evoked oscillations, comparing the tDCS after-effects with respective baseline measures showed for low-dosage tDCS over M1 a negative cluster over the occipito-parietal electrodes for the Alpha frequency band (α; POST30; $p = 0.021$, time-period: 53–155 ms after TMS), a further negative cluster over the frontal electrodes for the Beta frequency band (β; POST30; $p = 0.019$, time-period: 185–295 ms after TMS), and two negative clusters for the Gamma frequency band over the fronto-central (γ; POST0, $p = 0.012$, time-period: 52–98 ms after TMS) and centro-parietal electrodes (γ; POST30, $p = 0.038$, time-period 63–126 ms after TMS), Fig. 8A. For medium-dosage tDCS over M1, a positive cluster over the parietal electrodes (θ; POST30; $p = 0.024$, time-period: 60–125 ms after TMS) and another positive cluster over the frontal electrodes (β; POST30; $p = 0.019$, time-period: 185–295 ms after TMS) was observed, Fig. 8B. Furthermore, for high-dosage tDCS over M1, two negative clusters were identified over the occipital electrodes for the Theta frequency band, one at the POST0, and the other at the POST30 time-point (θ; POST0, $p = 0.018$, time-period: 65–118 ms after TMS; POST30, $p = 0.034$, time-period: 96–185 ms after TMS), as well as one negative cluster for the Alpha frequency band over the frontal electrodes (α; POST0, $p = 0.018$, time-period: 59–96 ms after TMS), two negative clusters for the Beta frequency band over the right fronto-central (β; POST0, $p = 0.032$, time-period: 54–83 ms after TMS), and right parietal electrodes (β; POST30, $p = 0.038$, time-period 93–164 ms after TMS), and one negative cluster for the Gamma frequency band over the central electrodes (γ; POST30, $p = 0.022$, time-period 87–196 ms after TMS), Fig. 8C. No significant clusters were however identified between sham measures and active M1 tDCS dosages.

For the distributed effects of ***tDCS over the PFC***, the cluster-based permutation tests comparing the tDCS after-effects with respective baseline measures showed for medium-dosage tDCS a negative cluster over the left centro-parietal electrodes for the Theta frequency band (θ; POST30; $p = 0.031$, time-period: 51–108 ms after TMS), a further negative cluster over the frontal

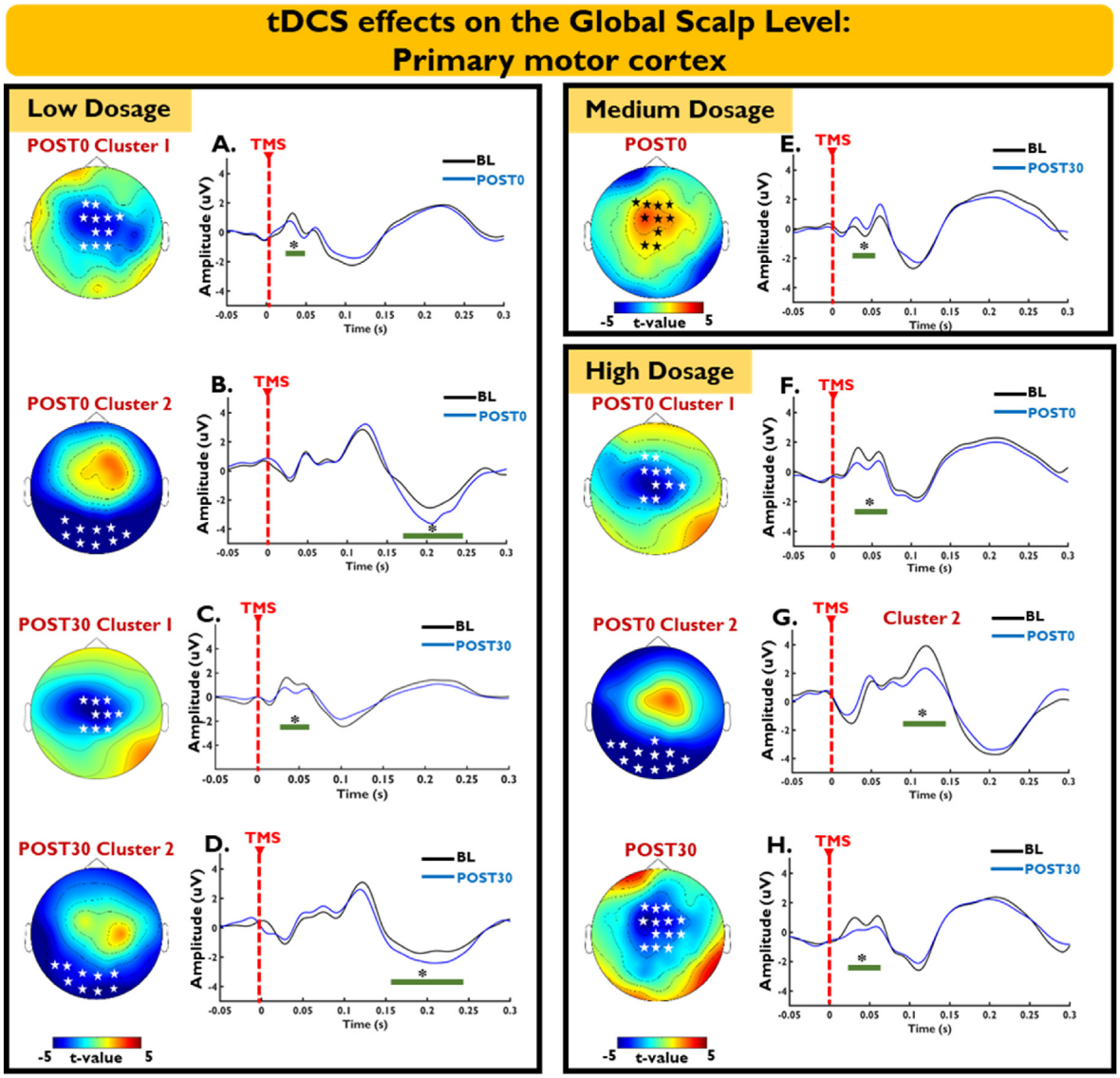

Fig. 4. Global effects of tDCS on TMS-evoked Potentials (over the M1; comparison vs. baseline). The distributed effects of tDCS were evaluated via cluster-based permutation tests, immediately (POST0) to up to 2 h after stimulation (POST30, POST60, POST120), over all electrodes. Topographic plots (distribution of the t-values) showing significant negative clusters (white stars) or positive clusters (black stars), together with the TEP deflections recorded over the EEG channels contribute to the significant clusters after low- (A–D), medium- (E) and high-dosage (F–H) tDCS over M1, and the green line represents the duration of the significant differences (*) between the respective time-points of tDCS- after effects vs. baseline. For further information regarding the specific electrodes forming each cluster refer to Table S8. See also figure S5 for the global effects of tDCS on TMS-evoked Potentials (over M1; comparison vs. Sham). (For interpretation of the references to color in this figure legend, the reader is referred to the Web version of this article.)

electrodes for the Alpha frequency band (α; POST30; p = 0.018, time-period: 75–213 ms after TMS), two negative clusters for the Beta frequency band over the right centro-frontal electrodes (β; POST0, p = 0.042, time-period 62–93 ms after TMS and POST30, p = 0.022, time-period 71–131 ms after TMS), as well as one negative cluster over the right frontal electrodes for the Gamma frequency band (γ; POST30; p = 0.014, time-period: 99–288 ms after TMS), Fig. 9B. For high-dosage tDCS, a negative cluster was identified over the right centro-frontal electrodes for the Alpha frequency band (α; POST0; p = 0.023, time-period: 89–201 ms after TMS), and two negative clusters for the Gamma frequency band over the fronto-central electrodes (γ; POST0; p = 0.029, time-period: 87–196 ms after TMS; POST30; p = 0.003, time-period: 67–116 ms after TMS), Fig. 9C. No significant clusters were however identified between sham measures and active PFC tDCS dosages.

Together, these results indicate widespread effects of tDCS on TMS-evoked oscillations at the global scalp level, which hints at the contribution of distant cortical networks to the overall tDCS effects.

3.2.5. tDCS-altered TMS-elicited MEPs

The 2-factorial rmANOVAs on ΔMEPs (normalized values and excluding baseline measures), revealed significant effects of the main factors condition and time-point and their respective interactions ($F_{(2.152,36.586)} = 3.094, p = 0.002, \eta_p^2 = 0.154$) (Table 7A, Fig. 10). Post hoc tests comparing after-effects of real with sham stimulation showed ΔMEP amplitude reductions after low- and high-dosage (both at POST0, POST30) tDCS (Fig. 10). In addition, the secondary rmANOVA (condition-4 levels, and time point-5 levels), conducted for the MEP amplitudes (absolute values) revealed significant main effects of time-point, and a significant 'condition × time-point' interaction ($F_{(1.550,26.534)} = 70.463, p < 0.001, \eta_p^2 = 0.806$) (Table 7B,

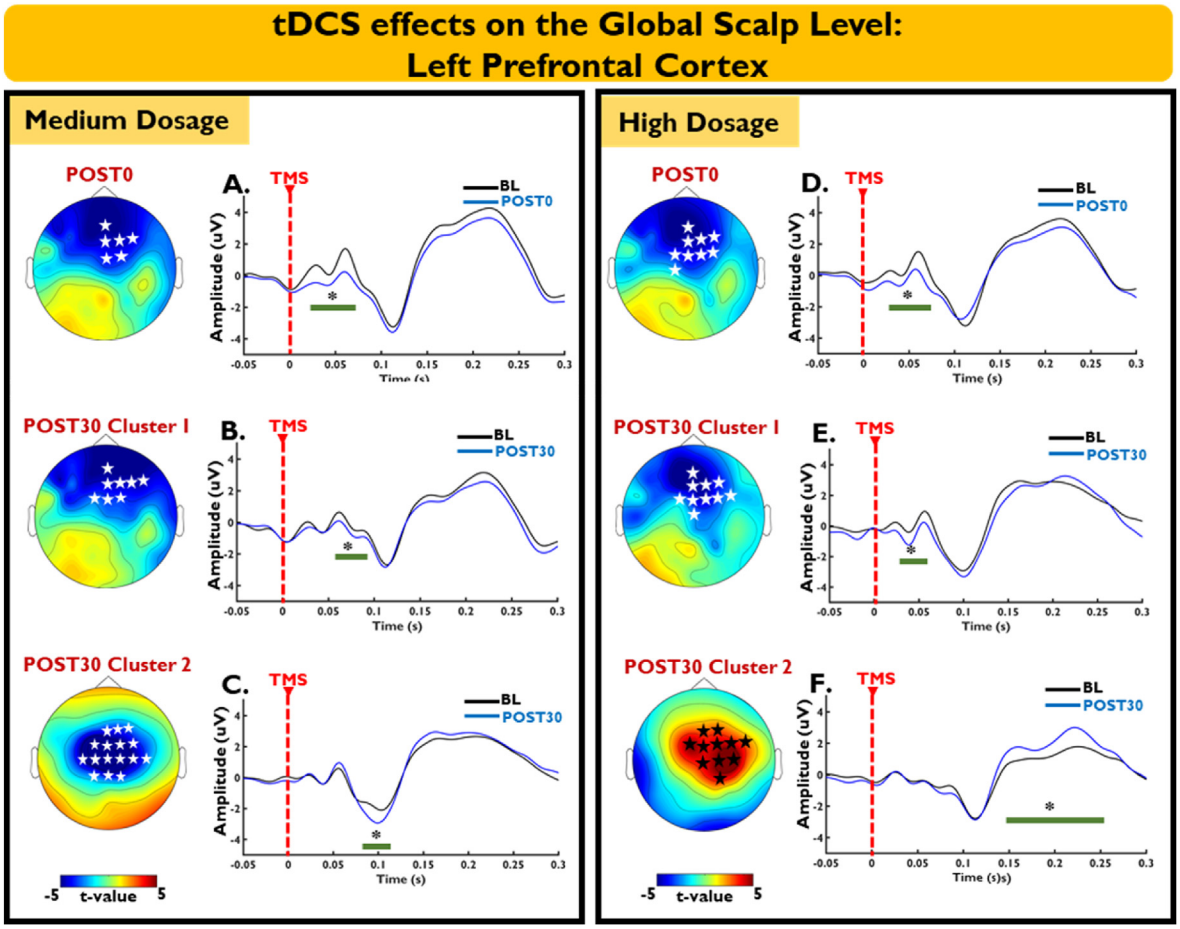

Fig. 5. Global effects of tDCS on TMS-evoked Potentials (over the PFC; comparison vs. baseline). The distributed effects of tDCS were evaluated, using cluster based permutation test, immediately (POST0) to up to 2 h after stimulation (POST30, POST60, POST120), over all electrodes. Topographic plots (distribution of the t-values) showing significant negative clusters (white stars) or positive clusters (black stars), together with the TEP deflections recorded over the EEG channels which constitute the significant cluster, after medium- (A–C), and high-dosage (D–F) tDCS over the prefrontal cortex. The green line represents the duration of the significant differences (*) between the respective time-points of tDCS-after effects vs. baseline. For further information regarding the specific electrodes forming each cluster refer to Table S8. See also Figure S5 for the global effects of tDCS on TMS-evoked Potentials (over PFC; comparison vs. Sham). (For interpretation of the references to color in this figure legend, the reader is referred to the Web version of this article.)

Figure S7). Post hoc tests comparing tDCS after-effects with respective baseline values revealed a significant MEP amplitude reduction after low- (POST0, POST30) and high-dosage (POST0, POST30 and POST60) tDCS (Figure S.7). In summary, the results show dosage-dependent effects of tDCS on MEP amplitude alterations, with low- and high-dosage tDCS resulting in a cortico-spinal excitability reduction, while medium-dosage tDCS had no effects.

3.3. Association between tDCS-altered TMS-evoked potentials and TMS-elicited MEPs and tDCS-induced electrical fields

The Pearson correlation results indicate a significant positive relation between P30 and MEP for low- (POST0: $r = 0.56$, $p = 0.031$), and high-dosage tDCS (POST0: $r = 0.53$, $p = 0.037$) (Fig. 11A). No significant correlations were found between other TEPs and MEPs across conditions and time-points (all with $p > 0.05$). There was a significant positive correlation between tDCS-induced EFs and MEP amplitude changes after high-dosage tDCS (POST30: $r = 0.51$, $p = 0.029$), indicating that subjects with higher EFs over the targeted area showed larger MEP amplitude changes (Fig. 11B). However, the correlation results did not show any significant relationship between tDCS-induced EFs and tDCS-altered TEP peaks (all with $p > 0.05$). Moreover, the tDCS-induced EFs over the PFC were significantly lower than the tDCS-induced EF over M1 ($p = 0.011$), Fig. 11C. Interestingly, tDCS-induced EFs over M1 and the PFC did not correlate significantly ($r = 0.31$, $p = 0.074$). Note that the tDCS-induced EFs were calculated using a GM mask over the TMS-induced effective EFs at each stimulation site (see respective section of the method).

In summary, the results showed an association between the early TEP peaks (only P30) and MEPs, which is in line with previous findings [33]. However, this was not consistent across all active conditions and for all respective time-points of tDCS-after-effects. Also, the regional tDCS-induced EF over the PFC is, on average and across participants, lower than that over M1, but this might not be identical at the individual level in each case. Note that the tDCS-induced EF estimation was done after the end of experiment as a post hoc analysis.

3.4. Qualitative assessment of tDCS protocols

The results of the Chi-square tests indicate no significant heterogeneity for any of the tDCS dosages (sham: $\chi2 = 0.111$, $p = 0.739$; low-dosage: $\chi2 = 2.778$, $p = 0.096$; medium-dosage: $\chi2 = 1.778$, $p = 0.182$; high-dosage: $\chi2 = 1.000$, $p = 0.317$), which shows successful blinding. Also, the ANOVAs conducted for the side-effects showed no significant effects either during or 24 h after stimulation (Table 8). Guesses of received stimulation intensity vs actual

Table 5
Results of the three-way ANOVAs conducted for tDCS-induced alterations of cortical oscillations (conducted with the normalized values). The three-way rmANOVAs conducted to test the effects of active tDCS conditions on TMS-evoked oscillations vs. sham showed no significant effects of neither the main factors condition, time-point, and stimulation sites, nor their respective interactions. For all ANOVAs, Mauchly's test of sphericity was conducted, and the Greenhouse-Geisser correction was applied when necessary. See also Table 6 for the results of the confirmatory two-way ANOVAs (for each stimulation site separately; conducted with the normalized values) and Table S9 and Table S10 for the three- and two-ways rmANOVAs (conducted with the absolute values) conducted for tDCS-induced TMS-evoked potentials. d.f. = degrees of freedom, η_p^2 = partial eta squared.

	Factors		d.f.	F Value	p Value	η_p^2
Frequency bands	Δθ	**Condition**	1.789, 19.680	2.318	0.129	0.174
		Time-point	3, 33	0.461	0.712	0.040
		Stimulation site	1, 12	4.016	0.067	0.213
		Condition × Time-point	3.610, 39.710	2.559	0.138	0.189
		Condition × Stimulation site	3, 33	0.971	0.418	0.081
		Time-point × Stimulation site	3, 33	0.174	0.913	0.016
		Condition × Time-point × Stimulation site	4.297, 47.269	0.560	0.827	0.048
	Δα	**Condition**	3, 24	0.334	0.801	0.040
		Time-point	3, 24	0.792	0.510	0.090
		Stimulation site	1, 12	2.236	0.169	0.148
		Condition × Time-point	2.031,16.252	2.139	0.149	0.211
		Condition × Stimulation site	3, 24	0.790	0.511	0.090
		Time-point × Stimulation site	1.290, 10.318	0.755	0.438	0.086
		Condition × Time-point × Stimulation site	1.495, 11.962	1.537	0.250	0.161
	Δβ	**Condition**	3, 33	0.716	0.550	0.061
		Time-point	1.664, 18.299	0.263	0.732	0.023
		Stimulation site	1, 11	1.535	0.241	0.122
		Condition × Time-point	1.783, 19.617	0.429	0.634	0.038
		Condition × Stimulation site	3, 33	1.223	0.317	0.100
		Time-point × Stimulation site	1.316, 14.481	1.133	0.324	0.093
		Condition × Time-point × Stimulation site	3.315, 29.856	0.720	0.501	0.085
	Δγ	**Condition**	3, 21	1.016	0.406	0.127
		Time-point	3, 21	0.784	0.516	0.101
		Stimulation site	1, 7	1.570	0.250	0.183
		Condition × Time-point	9, 63	1.201	0.310	0.146
		Condition × Stimulation site	3, 21	1.338	0.289	0.160
		Time-point × Stimulation site	3, 21	0.972	0.424	0.122
		Condition × Time-point × Stimulation site	9, 63	0.925	0.509	0.117

intensity are shown in Table S16. Ratings of the presence and intensity of side-effects are documented in S17.

4. Discussion

In this study, we explored the dosage-dependent neurophysiological effects of cathodal tDCS at two targeted stimulation sites, the left M1 and left PFC. In a single-blind and sham-controlled repeated measures design, four cathodal tDCS dosages of low, medium, high intensity, and sham stimulation were applied over the M1 and PFC. The after-effects were then tested by TMS-EEG and TMS-MEP techniques, at the regional and global scalp level, for TMS-evoked cortical reactivity, oscillations, and MEP amplitude alterations. In general, at the regional level, we observed a nonlinear dosage-dependent effect of M1 tDCS on TMS-evoked early positive TEPs, and MEPs, whereas PFC tDCS decreased almost uniformly the early positive TEP peaks; we however did not observe regional after-effects of tDCS on TMS-evoked oscillations. In addition, we

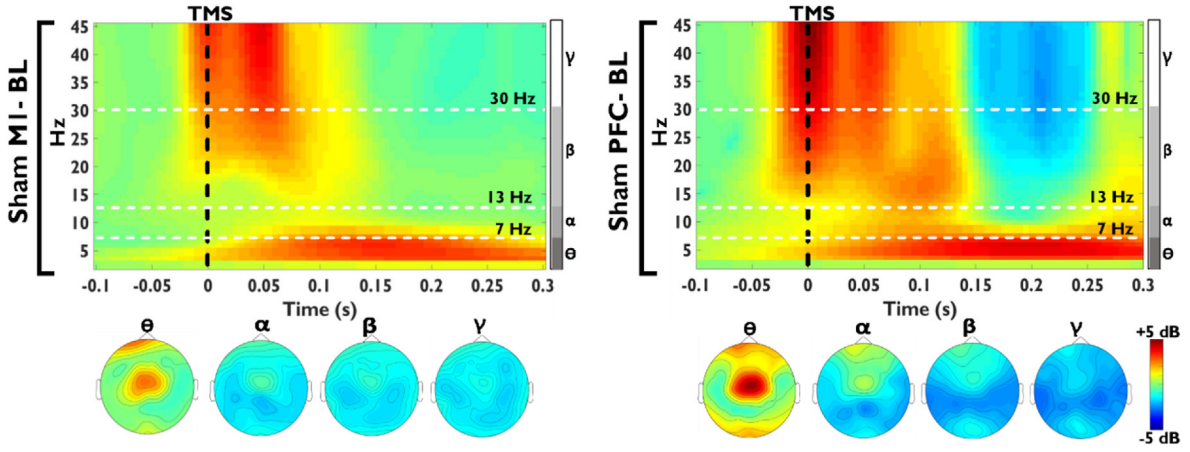

Fig. 6. Local reperesentation of TMS-evoked Oscillations. Time-frequency representations (TFRs) of oscillatory power (Morlet wavelet; wavelet width: starting from 2.6 cycles and adding 0.2 cycle for each 1 Hz), normalized (db) to the respective baseline (−500 to −100 ms), for ROI_{M1} (averaged FC1 and CP1 electrodes) and ROI_{PFC} (averaged FCz and Fz electrodes). The time-frequency plot shows the total power across different frequencies as a function of time following sham stimulation (baseline; BL) over the left primary motor cortex (ROI_{M1}; **left**) and left DLPFC (ROI_{PFC}; **right**). Power estimates were then calculated for four separate frequency bands, comprising Theta (θ; 4–7Hz), Alpha (α; 8–13Hz), Beta (β; 14–29Hz), and Gamma (γ; 30–45Hz), and a time window of 50–300 ms. The topographic plots are showing the power estimates across four different frequency bands for the sham condition over M1 (left) or PFC (right) for the baseline measures. Note that the time-frequency and topographic plots are only illustrated for the baseline measures of sham conditions, as there were no significant differences of the regional tDCS after-effects on TMS-evoked oscillations in comparison with baseline and/or sham values.

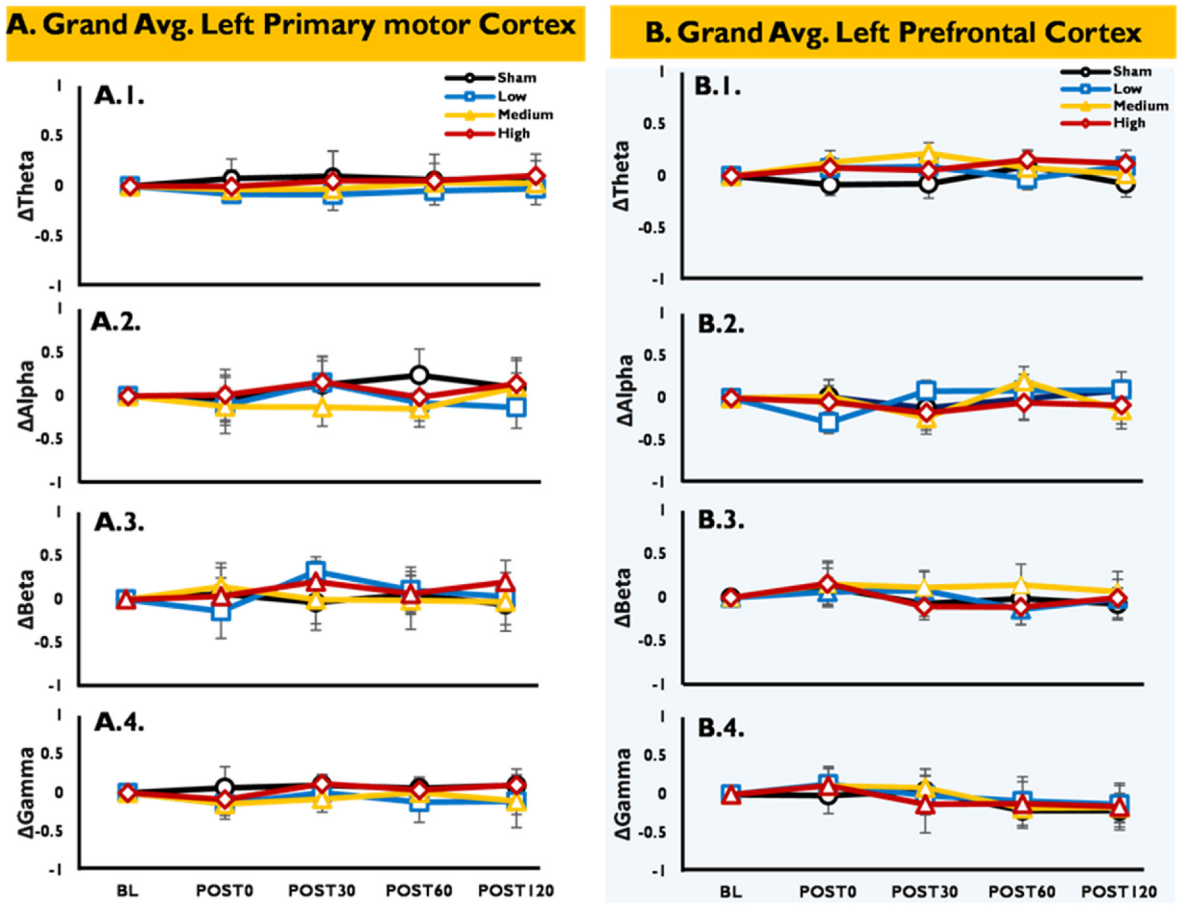

Fig. 7. Local effects of tDCS on TMS-evoked Oscillations (normalized values). Time-frequency representations (TFRs) of oscillatory power were calculated (Morlet wavelet; wavelet width: starting from 2.6 cycles and adding 0.2 cycle for each 1 Hz), and then normalized (db) to the respective baseline (−500 to −100 ms), for ROI_{M1} (averaged FC1 and CP1 electrodes) and ROI_{PFC} (averaged FCz and Fz electrodes). Then power estimates were calculated before (BL), and for four time-points (immediately: POST0, 30min: POST30, 60min: POST60 and 120min: POST120) after tDCS, for four separate frequency bands, including Theta (θ; 4–7Hz), Alpha (α; 8–13Hz), Beta (β; 14–29Hz) and Gamma (γ; 30–45Hz), within a time window of 50–300 ms. **A.1–4, B.1–4).** Finally, the baseline-normalized values were calculated. Error bars show the standard error of the mean (SEM). See figure S6 for the local effects of tDCS on TMS-evoked oscillations (absolute values).

observed relatively larger TEP amplitudes at baseline over M1 in comparison with PFC, which is line with previous findings [66,97–99] (Fig. 12). In the current study, we diminished the impact of these baseline differences by baseline standardization. Furthermore, at the global scalp level, we observed distributed effects of tDCS on both, TMS-evoked potentials and oscillations. Computational modeling of tDCS-induced EFs showed relatively lower EFs over the PFC in comparison with M1 with the respective electrode positions, which was reflected by relatively smaller physiological effects after PFC, as compared to M1 tDCS. Blinding was successful, and all participants tolerated tDCS well. These findings are discussed in detail below.

4.1. Effects of tDCS on TMS-evoked potentials, MEPs and oscillations (regional effects)

Previous TMS-EEG studies have suggested that the early P30 TEP peak might reflect excitatory processes at the stimulation site [44,86,100,101]. In addition, recent studies of our group have shown dosage-dependent non-linear cathodal ***tDCS after-effects over M1***, which are suggested to be linked with calcium channel dynamics [28,102]. These together might explain, at the regional level, the observed reduction of the P30 TEP peak after low (which is in line with previous studies [14,15]) and high dosage tDCS over M1, and an enhancement after medium dosage tDCS, which is also in accordance with the tDCS after-effects on MEP amplitude changes. Likewise, the alteration of the P60 peak, which is suggested to be controlled by fast glutamatergic neurotransmission in the stimulated cortical network [86,100,103–105], might be caused by the dependency of cathodal tDCS after-effects from glutamate, specifically the reduction of glutamate after low intensity cathodal tDCS, and the presumably glutamate-dependent calcium dynamics causing the after-effects of medium- and high-dosage tDCS [28,30,102,106], as the effects are equivalent to the P30 peak. However, alternative explanations cannot be ruled out, e.g. antagonistic responses of different cortical layers to an identical stimulation dosage [107,108]. At present, these explanations are speculative and should be explored directly in future studies.

A null effect of tDCS on late-latency peaks (at periods ~100 ms, and ~200 ms; e.g. N100 and P200) was observed. Previous studies have linked these peaks to changes of local GABA-related activity [103,109,110], as well as interhemispheric excitatory-inhibitory activity [86,100,109,111–114]. Therefore, it might be speculated that local GABA reduction, which would decrease this potential, would be counteracted upon by glutamate reduction-related enhancement of the N100, which would then result in a zero-net effect of tDCS on the N100. Sensory and somatosensory evoked potentials might also contribute to these late-latency peaks resulting from the TMS-elicited clicking noise and coil vibration [15,35,63,115,116], and diminish effect differences between sham

Table 6
Results of the confirmatory two-way ANOVAs conducted for tDCS-induced alterations of cortical oscillations (conducted with the normalized values). The two-way rmANOVAs conducted for each stimulation site separately to test the effects of active tDCS conditions on TMS-evoked oscillations vs. sham showed no significant effect of neither the main factors condition and time-point nor their respective interaction. For all ANOVAs, Mauchly's test of sphericity was conducted, and the Greenhouse-Geisser correction was applied when necessary. d.f. = degrees of freedom, η_p^2 = partial eta squared.

	Stimulation Site	Factors	d.f.	F Value	p Value	η_p^2
Δθ	M1	Condition	1.259, 16.372	0.530	0.517	0.039
		Time-point	3, 51	0.865	0.468	0.062
		Condition × Time-point	1.072, 13.937	0.748	0.411	0.054
	PFC	Condition	3, 51	0.944	0.429	0.068
		Time-point	1.773, 23.052	1.283	0.293	0.090
		Condition × Time-point	9, 153	1.622	0.117	0.111
Δα	M1	Condition	3, 51	0.444	0.723	0.039
		Time-point	3, 51	0.779	0.514	0.066
		Condition × Time-point	9, 153	0.815	0.604	0.069
	PFC	Condition	3, 51	0.594	0.624	0.062
		Time-point	3, 51	0.646	0.593	0.067
		Condition × Time-point	9, 153	1.944	0.155	0.181
Δβ	M1	Condition	3, 51	1.567	0.086	0.162
		Time-point	1.018, 14.246	1.288	0.276	0.084
		Condition × Time-point	1.077, 15.081	1.099	0.317	0.073
	PFC	Condition	3, 51	1.034	0.322	0.098
		Time-point	3, 51	1.642	0.199	0.130
		Condition × Time-point	9, 153	0.438	0.728	0.038
Δγ	M1	Condition	3, 51	0.538	0.660	0.051
		Time-point	3, 51	1.984	0.138	0.166
		Condition × Time-point	9, 153	1.080	0.385	0.097
	PFC	Condition	1.038, 11.413	1.617	0.230	0.128
		Time-point	3, 51	1.621	0.203	0.128
		Condition × Time-point	9, 153	1.526	0.137	0.124

and real stimulation conditions. Knowledge about the neurophysiological foundations of TEPs is however still rudimentary and warrants further investigation.

The same mechanisms as outlined above might also contribute to the after-effects of ***tDCS over the PFC***, but anatomical and/or neurophysiological differences might contribute to the gradual differences of the effects with respect to both cortical areas. The lower inter-electrode distance and larger scalp-to-cortex distance in case of prefrontal stimulation [36,37] resulted in lower tDCS-induced EFs over the PFC, as shown by computational results [21,38–40], and, therefore, potentially explains the observed uniform reduction of P30 and P60 after different dosages of tDCS over the PFC, in comparison with the observed dosage-dependent non-linear effects of tDCS over M1. Moreover, pharmacological studies showed that dopamine, which is more prevalent in the prefrontal, as compared to the motor cortex [41], strengthens the reduction of cathodal tDCS-generated cortical excitability diminution [117], and might thus have prevented the conversion effects of medium-dose tDCS into cortical excitability enhancement, as observed for the P30 amplitude after tDCS over M1.

The results, however, did not show any significant effects of tDCS on the regional TMS-evoked oscillations over both stimulation sites, which is in line with findings of other NIBS protocols [118].

4.2. Effects of tDCS on TMS-evoked potentials and oscillations (global scalp effects)

At the global scalp level, widespread effects across multiple EEG channels were observed for both, tDCS effects on TMS-evoked potentials and oscillations. This is in line with our computational modelling results showing spreading of tDCS-induced EFs from the stimulation site across remote regions, but also with previous findings, showing modulation of activity across functional cortical networks, as measured by EEG [119,120], and other neuroimaging techniques [121,122]. Interestingly, while we did not observe regional effects of tDCS for the late TEPs, the clusters revealed in the global scalp analysis suggest a contribution of these late-latency peaks to the distributed network which might be related to tDCS-altered GABA activity [109,123], additional to confounding factors explained above. These late-latency changes might also be secondary responses that reflect the regional effects at the stimulation site due to effective connectivity.

In addition, tDCS after-effects were observed on TMS-evoked oscillations across different frequency bands. Previous studies have suggested the β-band to be associated with motor [124], but also cognitive processes [125], and γ band oscillations are known to play a role in neuronal communication across cortical regions, as well as integration of sensory information [126,127]. With this in mind, GABA has been shown to play a role in modulation of γ and β activity [128,129], and the observed changes in the present study might likely be explained by the dependency of the tDCS after-effect on GABA modulation (Stagg et al., 2009). Given the mixed results of tDCS effects on neural oscillations, as seen in this study and the relevant literature [14–16,18], more research is clearly needed to better define any specific tDCS effects on TMS-evoked neural oscillations, and respective underlying mechanisms. Beyond these physiological considerations, however, it should be recognized that volume conduction effects cannot be ruled out [130].

4.3. Limitations and future directions

This study should be interpreted within the context of some limitations. First, the data were acquired from a relatively small sample over a couple of sessions involving different interventions. Thus, the results should be replicated in follow-up studies with larger samples. In addition, in the current study, the F3 position was selected to approximate the scalp location overlaying the left PFC [16,60]. TMS coil positioning based on MNI coordinates for targeting the left PFC would have increased exactness and should be preferred in future studies [56,131]. However, due to technical issues related to the used navigation system, we could not use this feature. Note that we used navigated TMS for both, M1 and PFC stimulation sites, to keep TMS coil positions constant between

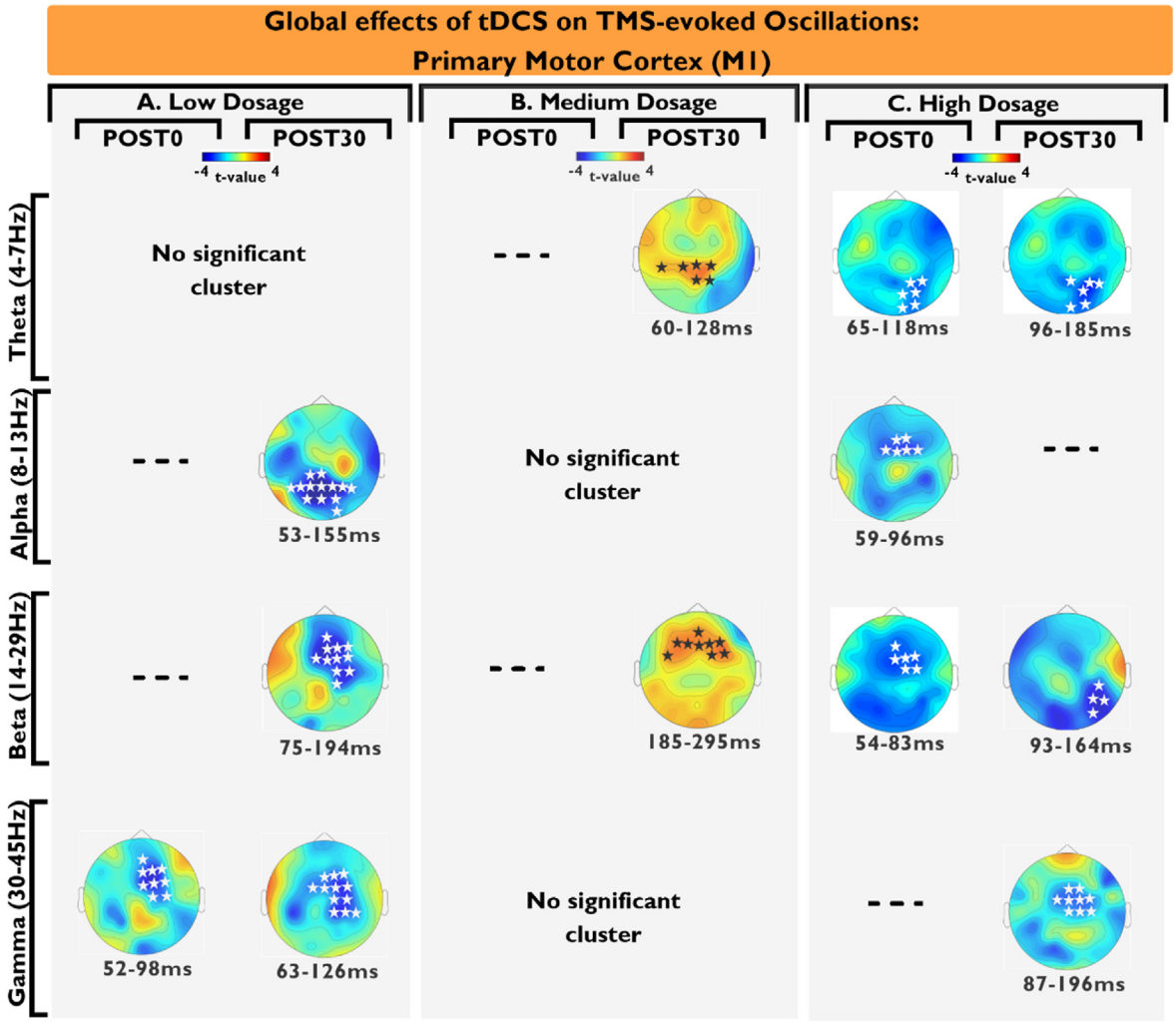

Fig. 8. Global effects of tDCS on TMS-evoked oscillations (tDCS over M1; comparison vs. baseline). The distributed effects of tDCS on oscillatory brain activity were evaluated by cluster-based permutation tests, immediately (POST0) to up to 2 h after stimulation (POST30, POST60, POST120), over all electrodes. Topographic plots (distribution of the t-values) show significant negative clusters (white stars) or positive clusters (black stars), over the EEG channels, which constitute significant clusters after low- (A), medium- (B), and high-dosage (C) tDCS for Theta, Alpha, Beta and Gamma frequency bands. The permutation tests were calculated within the time window of 50–300 ms after TMS. Significant clusters were identified only for POST0 and/or POST30. Dashed lines indicate no significant cluster at the respective time point. The duration below each topographic plot indicates the time period of the significant clusters. Further detailed information regarding the specific electrodes forming each cluster see Table S15.

sessions. Also, it would be advantageous to use a navigation system for tDCS and EEG electrode positioning in future studies. However, the lack of baseline MEP and TEP amplitude differences within stimulation sites and between sessions suggest the reliability of the used tDCS electrodes and navigated TMS coil positioning methods in this study.

In this study, we have used a specialized pipeline, with the aim to effectively minimize the respective artifact sources (e.g. TMS-evoked muscle artifacts over the PFC stimulation site) to uncover the underlying neural activity. While developing a unified TMS-EEG pipeline suited for all research questions is not trivial, recent studies have developed alternative preprocessing pipelines and demonstrated the impact of different artifact removal approaches on TMS-EEG outcomes, which should be considered in future studies (see these for details [58,75–77]). Furthermore, late-latency peaks (about 100 ms after the TMS pulse) might reflect also non-direct effects of TMS due to the contribution of auditory-evoked potentials resulting from the TMS clicking noise and bone-conducted sensory responses caused by coil vibration [15,35,63,115,116]. A recent study has suggested methods to reduce these confounding factors [64], which should be considered in future studies. In the present study, we did not use a thin layer of foam under the TMS coil, which could decrease the non-direct effects of TMS because of coil vibration, because this has the disadvantage of increasing RMT, and thus TMS intensity required for excitability measures because of the resulting larger coil to brain distance. This approach should however be considered in future studies. We have adjusted the TMS intensity to 100% of RMT as a compromise to receive reasonable TEP, but also reduce indirect TMS effects. For obtaining MEP, this stimulation intensity is however comparatively low and might have affected respective measures.

Moreover, in the current study, we used relatively large tDCS electrodes to evaluate the effect of conventional tDCS protocols. Several EEG electrodes over the targeted areas had, therefore, to be removed, which limits the selection of relevant EEG electrodes for the analysis of regional effects. Future studies might consider smaller and/or other relevant electrode montages, introduced in recent studies [16,18,132]. The selection of tDCS protocols in the current study was based on our previous study results of tDCS over

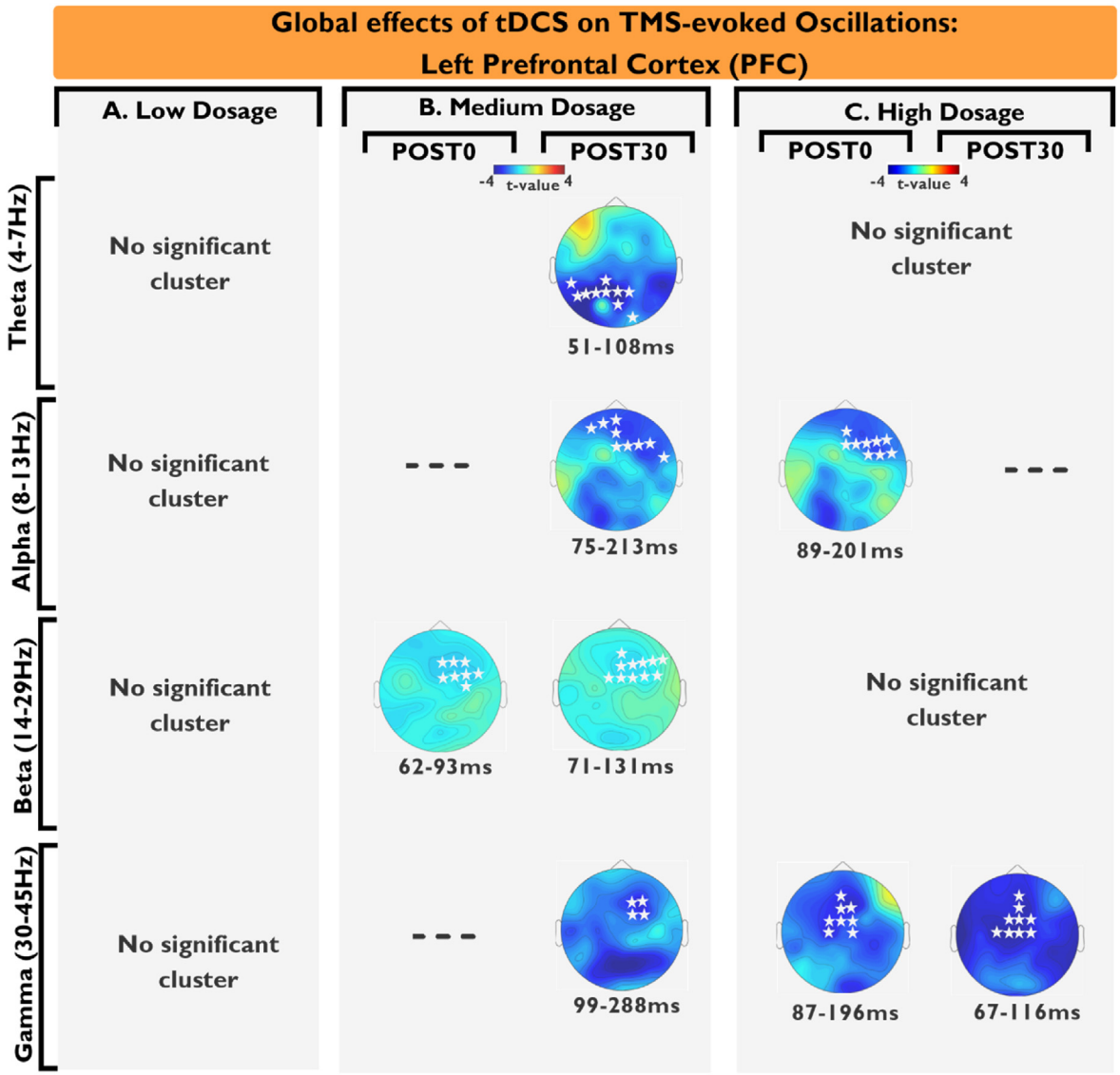

Fig. 9. Global effects of tDCS on TMS-evoked Oscillations (over the PFC; comparison vs. baseline). The distributed effects of tDCS on oscillatory brain activity were evaluated by cluster-based permutation tests, immediately (POST0) to up to 2 h after stimulation (POST30, POST60, POST120), over all electrodes. Topographic plots showing significant negative clusters (white stars) or positive clusters (black stars), over the EEG channels which constitute the significant clusters after low- (A), medium- (B), and high-dosage (C) tDCS for Theta, Alpha, Beta, and Gamma frequency bands. The permutation tests were calculated for a time window of 50–300 ms after TMS. Significant clusters were identified only after POST0 and/or POST30. Dashed lines indicate no significant cluster at the respective time point. The duration below each topographic plot indicates the time period of the significant clusters. For further detailed information regarding the specific electrodes forming each cluster refer to Table S15.

M1 [19]. We chose the protocols based on those which were most promising to reveal dosage-dependent non-linear effects, and thus our choice was effect-based. It included the lowest dosage used to induce an excitability diminution applied in that study (lowest intensity, and duration (15min)), a medium dosage, which induced excitability-enhancing effects (tDCS for 20min, medium intensity),

Table 7
Results of the ANOVAs conducted for evaluation of tDCS-generated alterations of TMS-evoked MEPs. The rmANOVA (**A**; normalized MEP values, baseline measures excluded from the analysis) showed significant effects of the main factors condition and time-point, and their respective interactions. In addition, the secondary rmANOVA (**B**; absolute values) results show a significant main effect of time-point, and a significant 'condition × time-point' interaction. Asterisks indicate significant effects ($p < 0.05$), d.f. = degrees of freedom, η_p^2 = partial eta squared.

	Factors		d.f.	F Value	p Value	η_p^2
A	**ΔMEP**	**Condition**	**3, 51**	**13.547**	**<0.001***	**0.443**
		Time-point	**1.586, 26.968**	**3.155**	**0.033***	**0.157**
		Condition × Time-point	**2.152, 36.586**	**3.094**	**0.002***	**0.154**
B	**MEP**	**Condition**	3, 51	1.212	0.315	0.067
		Time-point	**1.599, 27.157**	**78.668**	**<0.001***	**0.822**
		Condition × Time-point	**1.550, 26.534**	**70.463**	**<0.001***	**0.806**

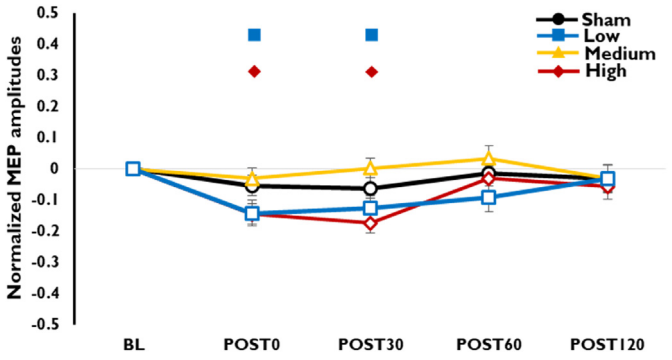

Fig. 10. Effects of tDCS on TMS-elicited MEPs (normalized values). Low, medium, and high cathodal tDCS intensities, and sham stimulation, were applied over the primary motor cortex (M1). The tDCS effects on cortico-spinal excitability were then evaluated immediately (POST0), and for up to 2 h after stimulation (POST30, POST60, POST120), using baseline-normalized ΔMEP amplitudes. Floating symbols show a significant difference of active tDCS conditions vs. sham. Error bars show the standard error of the mean (SEM).

and a high dosage, which induced excitability-diminishing effects (tDCS for 20min; high intensity). While blinding was efficient with respect to stimulation intensity, we cannot be sure that blinding was affected by stimulation duration, however identical stimulation durations were associated with different intensities.

Also, previous studies showed a relatively uniform enhancement of motor cortical excitability following different anodal tDCS dosages [20,133]. Therefore, the results of the current study might not directly translate to anodal stimulation effects, which needs further investigations. Indeed, a respective parallel study with an identical experimental design is currently conducted by our group. Likewise, pharmacological and neuroimaging studies highlighted polarity-dependent effects of tDCS on GABA and/or glutamatergic activities, among other receptors/neurotransmitters [30,106], which might link to the TEP peak alterations (as outlined above). The impact of tDCS on positive or negative TEPs might furthermore depend on the orientation of the tDCS-induced electrical field. To explore this, however, also anodal tDCS would have been required, which was out of the scope of this study, and needs further

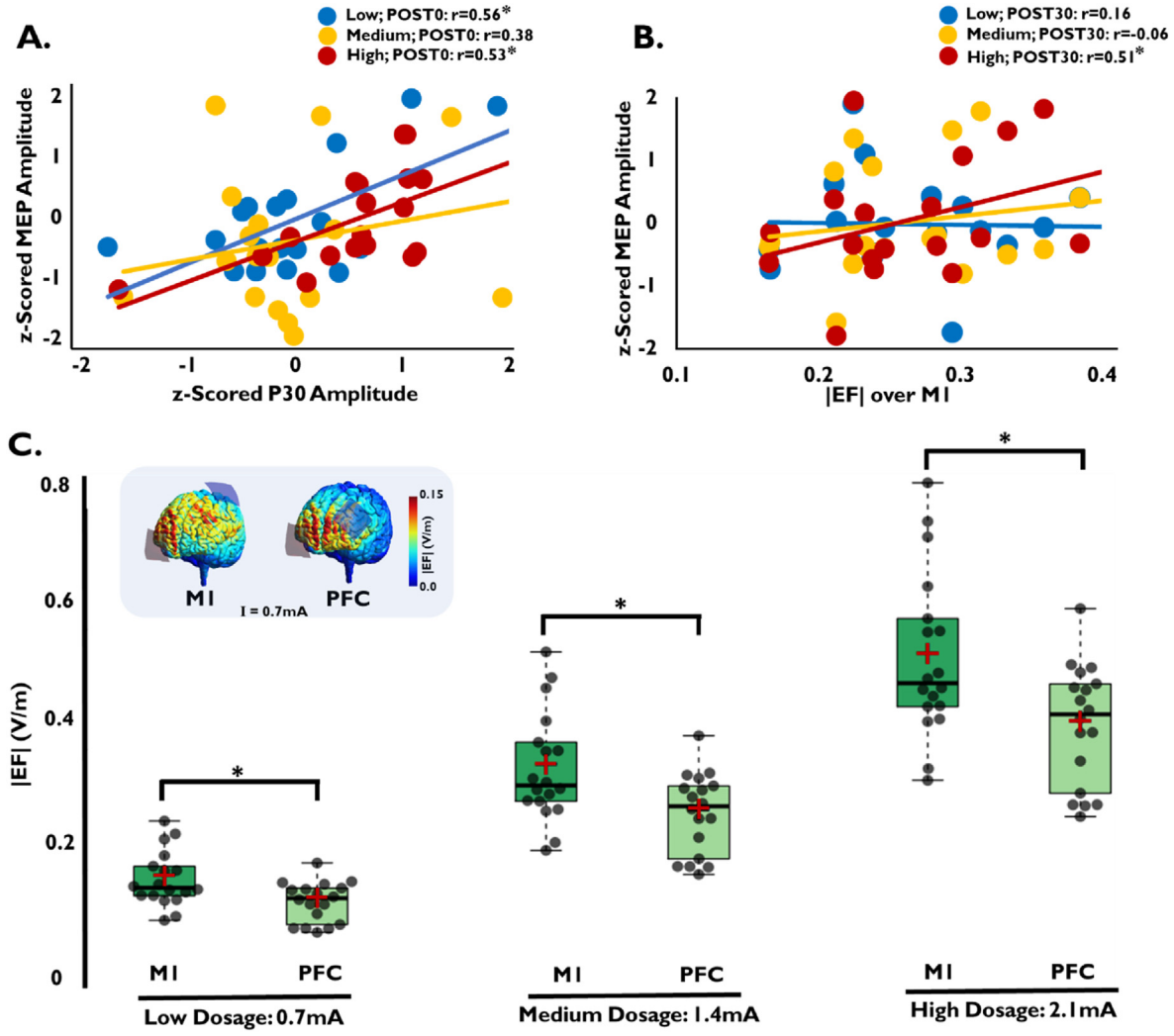

Fig. 11. Association between tDCS-generated TMS-evoked Potential and TMS-elicited MEP alterations and tDCS-induced electrical fields. Pearson correlations were calculated to test the relationship between tDCS-generated TEP and MEP alterations (A), tDCS-generated MEP alterations and tDCS-induced EF (B). In addition, the differences between the tDCS-induced EFs (strength |EF|) over the M1 and PFC were explored via paired Student's *t*-test (C: Box plots (whiskers extend to minimum and maximum individual values (shown in dark grey circles)); also the median (horizontal black line in the box), and means (shown as red + symbols) of the EFs are shown). Note that the estimated tDCS-induced EFs were calculated for low- (0.7 mA), medium- (1.4 mA), and high-intensity (2.1 mA) tDCS, but that the results can linearly be scaled for the other tDCS intensities based on a single intensity according to the quasi-static approximation [91]. The colors of the anatomical pictures are illustrating EF magnitudes induced by tDCS (I = 0.7 mA) estimated via SimNIBS open-source software with its default parameters and head model (ernie.msh); for individual EF maps see Figure S8 and Figure S9. Asterisks show significant differences. (For interpretation of the references to color in this figure legend, the reader is referred to the Web version of this article.)

Table 8
The presence and intensity of side effects were analyzed by one-way repeated-measure ANOVAs. No significant effects of side effects were identified either during or 24 h after stimulation. d.f. = degrees of freedom. η_p^2 = partial eta squared. Guesses of received stimulation intensity vs actual intensity are shown in Table S6. Ratings of the presence and intensity of side-effects are documented in Table S17.

	Side-effects	d.f	F Value	η_p^2	p Value
During stimulation	**Visual Phenomena**	7, 119	1.567	0.084	0.152
	Itching	7, 119	0.765	0.043	0.618
	Tingling	7, 119	1.780	0.095	0.098
	Pain	3.106, 52.800	1.041	0.058	0.384
24 h after stimulation	**Redness**	7, 119	0.363	0.021	0.922
	Headache	2.432, 41.342	1.157	0.064	0.332
	Fatigue	7, 119	1.560	0.084	0.154
	Concentration	3.038, 51.650	1.129	0.062	0.346
	Nervousness	3.100, 52.706	2.209	0.115	0.096
	Sleep Problem	7, 119	1.630	0.087	0.133

investigations. Moreover, the effects found in the present study are all at the neurophysiological level and obtained in healthy humans. Transferability to other cortical areas, other populations, such as elderly [134,135], as well as respective tDCS effects on cognitive and/or motor functions should not be taken for granted, and therefore be tested in future studies directly. Moreover, it would be relevant to explore to which level individual physiological responses allow to predict behavioral and cognitive outcomes. This might pave the way for future individual dosage adaptation in clinical applications.

Finally, the different effects obtained by prefrontal and motor cortex stimulation, as identified in this study, should be carefully evaluated in future studies, as it is not clear if these are due to biological differences between respective areas, or different current

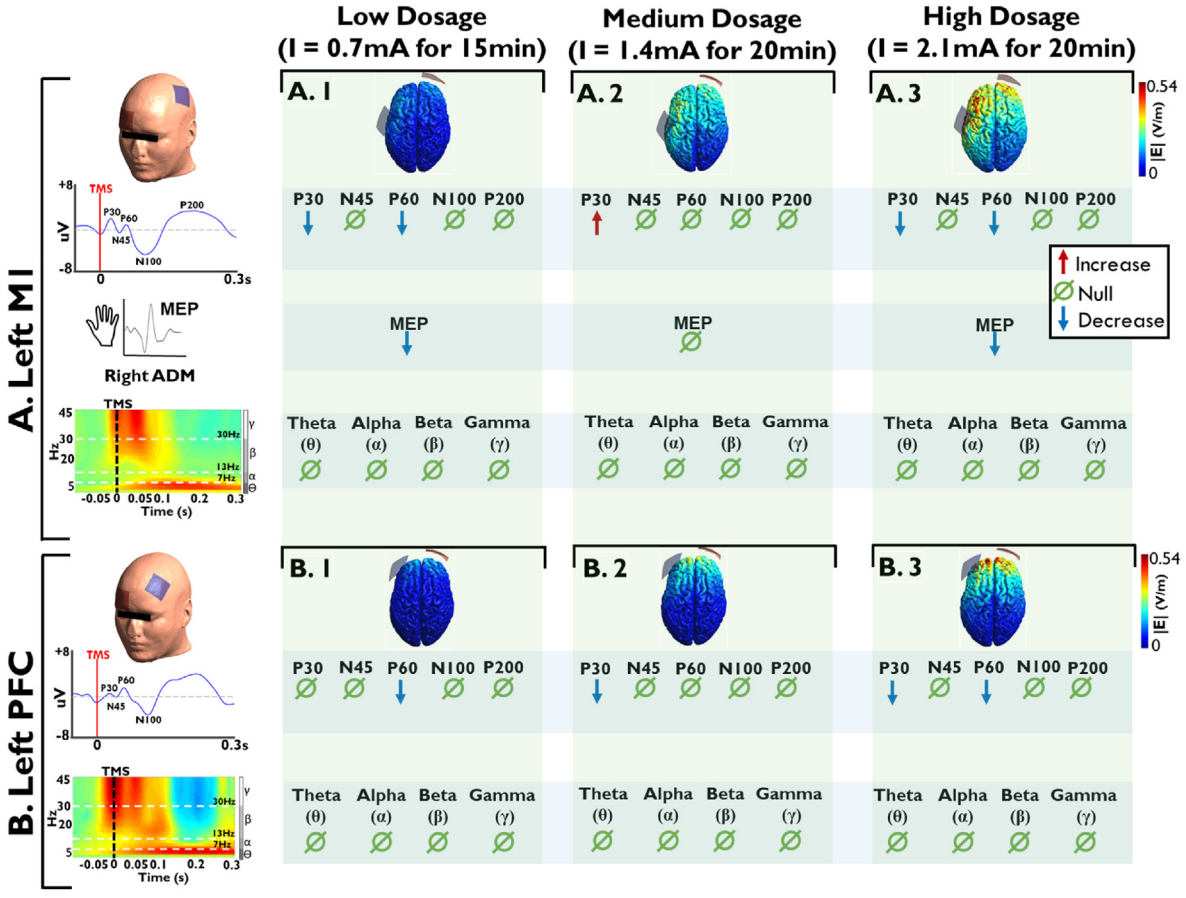

Fig. 12. Summary of the regional effects of different tDCS dosages on TMS-cortical reactivity and oscillations. Four cathodal tDCS dosages of low, medium, high intensity, and sham stimulation were applied over the left M1 (A.) and left PFC (B.). The after-effects were then tested by TMS-EEG and TMS-MEP techniques, for TMS-evoked cortical reactivity, oscillations, and MEP amplitude alterations. In general, at the regional level, we observed a nonlinear dosage-dependent effect of M1 tDCS on TMS-evoked early positive TEPs (P30 and P60; second row in A), and MEPs (third row in A), whereas PFC tDCS decreased almost uniformly the early positive TEP peaks (P30 and P60); we, however, did not observe regional after-effects of tDCS on TMS-evoked oscillations (fourth and third row in A and B, respectively). Colors in the cortical grey matter are illustrating electric field magnitudes induced by tDCS (first row in A and B; low dosage 0.7 mA; medium dosage: 1.4 mA, and high dosage: 2.1 mA) estimated via SimNIBS open-source software with its default parameters and head model (erni.msh) [49]. The blue downwards directed arrow, and the red upwards directed arrows indicate excitability reduction and enhancement in comparison to the respective sham and/or baseline values. The null sign represents no significant effects of tDCS on the respective measures in comparison to sham and/or baseline. (For interpretation of the references to color in this figure legend, the reader is referred to the Web version of this article.)

densities at the cortical level, due to anatomical differences. Further work, including computational modeling, might help to clarify this issue.

5. Conclusion

The results of this study show neurophysiological effects of motor cortex tDCS at the regional and global scalp level on TMS-evoked cortical reactivity, which are comparable with respective cortico-spinal excitability effects, measured by TMS-generated MEP. Low- and high-dosage motor cortex tDCS reduced the early positive TEP peak and MEP amplitudes, whereas an amplitude enhancement was observed for the medium dosage of motor cortex tDCS. In contrast, prefrontal low-, medium- and high-dosage tDCS almost uniformly reduced the early positive TEP peak amplitudes. Furthermore, over both cortical areas, regional modulatory effects of tDCS were not observed for late TEP, and TMS-evoked oscillations. However, at the global scalp level, the results suggest a distributed effect of tDCS on both, TMS-evoked potentials and oscillations. The specific differences of the effects of tDCS might be related to physiological, anatomical, and receptor and transmitter differences of motor and non-motor areas. The overall results provide the first direct comparison of tDCS effects over different brain areas at the physiological level, which will further consolidate the rationale for extending tDCS applications at both basic and clinical levels.

Funding

This work was supported by a research grant from the German Federal Ministry of Education and Research (BMBF) (GCBS grant 01EE1501). TP Mutanen has been funded by the Academy of Finland, Finland (Grant No. 321631).

CRediT authorship contribution statement

Mohsen Mosayebi-Samani: Conceptualization, Data curation, Formal analysis, Investigation, Writing – original draft, Visualization, Writing – review & editing. **Desmond Agboada:** Data curation, Formal analysis, Writing – review & editing. **Tuomas P. Mutanen:** Conceptualization, Formal analysis, Validation, Writing – review & editing. **Jens Haueisen:** Conceptualization, Supervision, Formal analysis, Methodology, Validation, Writing – review & editing. **Min-Fang Kuo:** Conceptualization, Project administration, Supervision, Formal analysis, Methodology, Validation, Writing – review & editing. **Michael A. Nitsche:** Conceptualization, Funding acquisition, Supervision, Formal analysis, Methodology, Validation, Writing – review & editing.

Declaration of competing interest

The authors declare the following financial interests/personal relationships which may be considered as potential competing interests: MA Nitsche is member of the Scientific Advisory Board of Neuroelectrics. None of the remaining authors have potential conflicts of interest to be disclosed.This work was supported by a research grant from the German Federal Ministry of Education and Research (BMBF) (GCBS grant 01EE1501). TP Mutanen has been funded by the Academy of Finland (Grant No. 321631).

Acknowledgment

We thank Prof. Marcello Massimini, Dr. Silvia Casarotto, and Dr. Matteo Fecchio for their important comments on the manuscript, and Dr. Asif Jamil, Dr. Fatemeh Yavari, Tobias Blanke, and Nina Abich for their valuable support during the study.

Appendix A. Supplementary data

Supplementary data to this article can be found online at https://doi.org/10.1016/j.brs.2023.02.010.

References

[1] Nitsche MA, Paulus W. Excitability changes induced in the human motor cortex by weak transcranial direct current stimulation. J Physiol 2000;527(3):633–9.
[2] Nitsche MA, Paulus W. Sustained excitability elevations induced by transcranial DC motor cortex stimulation in humans. Neurology 2001;57(10):1899–901.
[3] Nitsche MA, Nitsche MS, Klein CC, Tergau F, Rothwell JC, Paulus W. Level of action of cathodal DC polarisation induced inhibition of the human motor cortex. Clin Neurophysiol 2003;114(4):600–4.
[4] Yavari F, Jamil A, Mosayebi Samani M, Vidor LP, Nitsche MA. Basic and functional effects of transcranial Electrical Stimulation (tES)—an introduction. Neurosci Biobehav Rev 2018;85:81–92.
[5] Lefaucheur JP, Antal A, Ayache SS, Benninger DH, Brunelin J, Cogiamanian F, et al. Evidence-based guidelines on the therapeutic use of transcranial direct current stimulation (tDCS). Clin Neurophysiol : official journal of the International Federation of Clinical Neurophysiology 2017;128(1):56–92.
[6] Matsunaga K, Nitsche MA, Tsuji S, Rothwell JC. Effect of transcranial DC sensorimotor cortex stimulation on somatosensory evoked potentials in humans. Clin Neurophysiol : official journal of the International Federation of Clinical Neurophysiology 2004;115(2):456–60.
[7] Dieckhöfer A, Waberski TD, Nitsche M, Paulus W, Buchner H, Gobbelé R. Transcranial direct current stimulation applied over the somatosensory cortex – differential effect on low and high frequency SEPs. Clin Neurophysiol 2006;117(10):2221–7.
[8] Antal A, Kincses TZ, Nitsche MA, Bartfai O, Paulus W. Excitability changes induced in the human primary visual cortex by transcranial direct current stimulation: direct electrophysiological evidence. Investig Ophthalmol Vis Sci 2004;45(2):702–7.
[9] Kuo M-F, Chen P-S, Nitsche MA. The application of tDCS for the treatment of psychiatric diseases. Int Rev Psychiatr 2017;29(2):146–67.
[10] Dedoncker J, Brunoni AR, Baeken C, Vanderhasselt M-A. A systematic review and meta-analysis of the effects of transcranial direct current stimulation (tDCS) over the dorsolateral prefrontal cortex in healthy and neuropsychiatric samples: influence of stimulation parameters. Brain Stimul 2016;9(4):501–17.
[11] Nitsche M, Koschack J, Pohlers H, Hullemann S, Paulus W, Happe S. Effects of frontal transcranial direct current stimulation on emotional state and processing in healthy humans. Front Psychiatr 2012;3(58).
[12] Karuza EA, Balewski ZZ, Hamilton RH, Medaglia JD, Tardiff N, Thompson-Schill SL. Mapping the parameter space of tDCS and cognitive control via manipulation of current polarity and intensity. Front Hum Neurosci 2016;10(665).
[13] Tremblay S, Rogasch NC, Premoli I, Blumberger DM, Casarotto S, Chen R, et al. Clinical utility and prospective of TMS–EEG. Clin Neurophysiol 2019;130(5):802–44.
[14] Pellicciari MC, Brignani D, Miniussi C. Excitability modulation of the motor system induced by transcranial direct current stimulation: a multimodal approach. Neuroimage 2013;83:569–80.
[15] Ahn S, Fröhlich F. Pinging the brain with transcranial magnetic stimulation reveals cortical reactivity in time and space. Brain Stimul 2021;14(2):304–15.
[16] Hill AT, Rogasch NC, Fitzgerald PB, Hoy KE. Effects of prefrontal bipolar and high-definition transcranial direct current stimulation on cortical reactivity and working memory in healthy adults. Neuroimage 2017;152:142–57.
[17] Hill AT, Rogasch NC, Fitzgerald PB, Hoy KE. Impact of concurrent task performance on transcranial direct current stimulation (tDCS)-Induced changes in cortical physiology and working memory. Cortex 2019;113:37–57.
[18] Gordon PC, Zrenner C, Desideri D, Belardinelli P, Zrenner B, Brunoni AR, et al. Modulation of cortical responses by transcranial direct current stimulation of dorsolateral prefrontal cortex: a resting-state EEG and TMS-EEG study. Brain Stimul 2018;11(5):1024–32.
[19] Mosayebi Samani M, Agboada D, Jamil A, Kuo M-F, Nitsche MA. Titrating the neuroplastic effects of cathodal transcranial direct current stimulation (tDCS) over the primary motor cortex. Cortex 2019;119:350–61.
[20] Agboada D, Mosayebi Samani M, Jamil A, Kuo M-F, Nitsche MA. Expanding the parameter space of anodal transcranial direct current stimulation of the primary motor cortex. Sci Rep 2019;9(1):18185.
[21] Mosayebi-Samani M, Jamil A, Salvador R, Ruffini G, Haueisen J, Nitsche MA. The impact of individual electrical fields and anatomical factors on the neurophysiological outcomes of tDCS: a TMS-MEP and MRI study. Brain Stimul 2021;14(2):316–26.

[22] Laakso I, Mikkonen M, Koyama S, Hirata A, Tanaka S. Can electric fields explain inter-individual variability in transcranial direct current stimulation of the motor cortex? Sci Rep 2019;9(1):626.
[23] Yang D, Wang Q, Xu C, Fang F, Fan J, Li L, et al. Transcranial direct current stimulation reduces seizure frequency in patients with refractory focal epilepsy: a randomized, double-blind, sham-controlled, and three-arm parallel multicenter study. Brain Stimul 2020;13(1):109–16.
[24] Sudbrack-Oliveira P, Barbosa MZ, Thome-Souza S, Razza LB, Gallucci-Neto J, da Costa Lane Valiengo L, et al. Transcranial direct current stimulation (tDCS) in the management of epilepsy: a systematic review. Seizure 2021;86:85–95.
[25] Marceglia S, Mrakic-Sposta S, Fumagalli M, Ferrucci R, Mameli F, Vergari M, et al. Cathodal transcranial direct current stimulation improves focal hand dystonia in musicians: a two-case study. Front Neurosci 2017;11:508.
[26] Ishikuro K, Dougu N, Nukui T, Yamamoto M, Nakatsuji Y, Kuroda S, et al. Effects of transcranial direct current stimulation (tDCS) over the frontal polar area on motor and executive functions in Parkinson's disease; A pilot study. Front Aging Neurosci 2018;10:231.
[27] Batsikadze G, Moliadze V, Paulus W, Kuo MF, Nitsche M. Partially non-linear stimulation intensity-dependent effects of direct current stimulation on motor cortex excitability in humans. J Physiol 2013;591(7):1987–2000.
[28] Mosayebi-Samani M, Melo L, Agboada D, Nitsche MA, Kuo M-F. Ca2+ channel dynamics explain the nonlinear neuroplasticity induction by cathodal transcranial direct current stimulation over the primary motor cortex. Eur Neuropsychopharmacol 2020;38:63–72.
[29] Nitsche MA, Muller-Dahlhaus F, Paulus W, Ziemann U. The pharmacology of neuroplasticity induced by non-invasive brain stimulation: building models for the clinical use of CNS active drugs. J Physiol 2012;590(19):4641–62.
[30] Nitsche M, Fricke K, Henschke U, Schlitterlau A, Liebetanz D, Lang N, et al. Pharmacological modulation of cortical excitability shifts induced by transcranial direct current stimulation in humans. J Physiol 2003;553(1):293–301.
[31] Misonou H, Mohapatra DP, Park EW, Leung V, Zhen D, Misonou K, et al. Regulation of ion channel localization and phosphorylation by neuronal activity. Nat Neurosci 2004;7(7):711–8.
[32] Opie GM, Rogasch NC, Goldsworthy MR, Ridding MC, Semmler JG. Investigating TMS-EEG indices of long-interval intracortical inhibition at different interstimulus intervals. Brain Stimul 2017;10(1):65–74.
[33] Mäki H, Ilmoniemi RJ. The relationship between peripheral and early cortical activation induced by transcranial magnetic stimulation. Neurosci Lett 2010;478(1):24–8.
[34] Rogasch NC, Daskalakis ZJ, Fitzgerald PB. Mechanisms underlying long-interval cortical inhibition in the human motor cortex: a TMS-EEG study. J Neurophysiol 2013;109(1):89–98.
[35] Biabani M, Fornito A, Coxon JP, Fulcher BD, Rogasch NC. The correspondence between EMG and EEG measures of changes in cortical excitability following transcranial magnetic stimulation. J Physiol 2021;599(11):2907–32.
[36] Kozel FA, Nahas Z, deBrux C, Molloy M, Lorberbaum JP, Bohning D, et al. How coil-cortex distance relates to age, motor threshold, and antidepressant response to repetitive transcranial magnetic stimulation. J Neuropsychiatry Clin Neurosci 2000;12(3):376–84.
[37] McConnell KA, Nahas Z, Shastri A, Lorberbaum JP, Kozel FA, Bohning DE, et al. The transcranial magnetic stimulation motor threshold depends on the distance from coil to underlying cortex: a replication in healthy adults comparing two methods of assessing the distance to cortex. Biol Psychiatr 2001;49(5):454–9.
[38] Faria P, Hallett M, Miranda PC. A finite element analysis of the effect of electrode area and inter-electrode distance on the spatial distribution of the current density in tDCS. J Neural Eng 2011;8(6):066017.
[39] Laakso I, Tanaka S, Koyama S, De Santis V, Hirata A. Inter-subject variability in electric fields of motor cortical tDCS. Brain Stimul 2015;8(5):906–13.
[40] Opitz A, Paulus W, Will S, Antunes A, Thielscher A. Determinants of the electric field during transcranial direct current stimulation. Neuroimage 2015;109:140–50.
[41] Gaspar P, Bloch B, Le Moine C. D1 and D2 receptor gene expression in the rat frontal cortex: cellular localization in different classes of efferent neurons. Eur J Neurosci 1995;7(5):1050–63.
[42] Zilles K, Palomero-Gallagher N. Multiple transmitter receptors in regions and layers of the human cerebral cortex. Front Neuroanat 2017;11:78.
[43] Faul F, Erdfelder E, Buchner A, Lang A-G. Statistical power analyses using G*Power 3.1: tests for correlation and regression analyses. Behav Res Methods 2009;41(4):1149–60.
[44] Rogasch NC, Zipser C, Darmani G, Mutanen TP, Biabani M, Zrenner C, et al. The effects of NMDA receptor blockade on TMS-evoked EEG potentials from prefrontal and parietal cortex. Sci Rep 2020;10(1):3168.
[45] Ozdemir RA, Boucher P, Fried PJ, Momi D, Jannati A, Pascual-Leone A, et al. Reproducibility of cortical response modulation induced by intermittent and continuous theta-burst stimulation of the human motor cortex. Brain Stimul 2021;14(4):949–64.
[46] Oldfield RC. The assessment and analysis of handedness: the Edinburgh inventory. Neuropsychologia 1971;9(1):97–113.
[47] Bikson M, Grossman P, Thomas C, Zannou AL, Jiang J, Adnan T, et al. Safety of transcranial direct current stimulation: evidence based update 2016. Brain Stimul 2016;9(5):641–61.
[48] Rossi S, Hallett M, Rossini PM, Pascual-Leone A, Group SoTC. Safety, ethical considerations, and application guidelines for the use of transcranial magnetic stimulation in clinical practice and research. Clin Neurophysiol 2009;120(12):2008–39.
[49] Thielscher A, Antunes A, Saturnino GB. Field modeling for transcranial magnetic stimulation: a useful tool to understand the physiological effects of TMS? Conf Proc : Annual International Conference of the IEEE Engineering in Medicine and Biology Society IEEE Engineering in Medicine and Biology Society Annual Conference 2015;2015:222–5.
[50] Awiszus F, Borckardt J. TMS motor threshold assessment tool 2.0 2012. 2012. Available from: . [Accessed 19 October 2012].
[51] Awiszus F, Borckardt J. TMS motor threshold assessment tool (MTAT 2.0). USA: Brain Stimulation Laboratory, Medical University of South Carolina; 2011.
[52] Julkunen P. Mobile application for adaptive threshold hunting in transcranial magnetic stimulation. IEEE Trans Neural Syst Rehabil Eng : a publication of the IEEE Engineering in Medicine and Biology Society 2019;27(8):1504–10.
[53] Awiszus F. Chapter 2 TMS and threshold hunting. In: Paulus W, Tergau F, Nitsche MA, Rothwell JG, Ziemann U, Hallett M, editors. Supplements to clinical neurophysiology. Elsevier; 2003. p. 13–23.
[54] Tranulis C, Guéguen B, Pham-Scottez A, Vacheron MN, Cabelguen G, Costantini A, et al. Motor threshold in transcranial magnetic stimulation: comparison of three estimation methods. Neurophysiol Clin 2006;36(1):1–7.
[55] Awiszus F. Fast estimation of transcranial magnetic stimulation motor threshold: is it safe? Brain Stimul 2011;4(1):58–9. discussion 60-3.
[56] Fitzgerald PB. Targeting repetitive transcranial magnetic stimulation in depression: do we really know what we are stimulating and how best to do it? Brain Stimul 2021;14(3):730–6.
[57] Desforges M, Hadas I, Mihov B, Morin Y, Rochette Braün M, Lioumis P, et al. Dose-response of intermittent theta burst stimulation of the prefrontal cortex: a TMS-EEG study. Clin Neurophysiol 2022;136:158–72.
[58] Bertazzoli G, Esposito R, Mutanen TP, Ferrari C, Ilmoniemi RJ, Miniussi C, et al. The impact of artifact removal approaches on TMS–EEG signal. Neuroimage 2021;239:118272.
[59] Beam W, Borckardt JJ, Reeves ST, George MS. An efficient and accurate new method for locating the F3 position for prefrontal TMS applications. Brain Stimul 2009;2(1):50–4.
[60] Herwig U, Satrapi P, Schonfeldt-Lecuona C. Using the international 10-20 EEG system for positioning of transcranial magnetic stimulation. Brain Topogr 2003;16(2):95–9.
[61] Lioumis P, Kicic D, Savolainen P, Makela JP, Kahkonen S. Reproducibility of TMS-Evoked EEG responses. Hum Brain Mapp 2009;30(4):1387–96.
[62] Mutanen T, Maki H, Ilmoniemi RJ. The effect of stimulus parameters on TMS-EEG muscle artifacts. Brain Stimul 2013;6(3):371–6.
[63] Conde V, Tomasevic L, Akopian I, Stanek K, Saturnino GB, Thielscher A, et al. The non-transcranial TMS-evoked potential is an inherent source of ambiguity in TMS-EEG studies. Neuroimage 2019;185:300–12.
[64] Rocchi L, Di Santo A, Brown K, Ibáñez J, Casula E, Rawji V, et al. Disentangling EEG responses to TMS due to cortical and peripheral activations. Brain Stimul 2021;14(1):4–18.
[65] Rosanova M, Casali A, Bellina V, Resta F, Mariotti M, Massimini M. Natural frequencies of human corticothalamic circuits. J Neurosci 2009;29(24):7679–85.
[66] Fecchio M, Pigorini A, Comanducci A, Sarasso S, Casarotto S, Premoli I, et al. The spectral features of EEG responses to transcranial magnetic stimulation of the primary motor cortex depend on the amplitude of the motor evoked potentials. PLoS One 2017;12(9):e0184910 [-e].
[67] McFadden JL, Borckardt JJ, George MS, Beam W. Reducing procedural pain and discomfort associated with transcranial direct current stimulation. Brain Stimul 2011;4(1):38–42.
[68] Nitsche MA, Cohen LG, Wassermann EM, Priori A, Lang N, Antal A, et al. Transcranial direct current stimulation: state of the art 2008. Brain Stimul 2008;1(3):206–23.
[69] Nikouline V, Ruohonen J, Ilmoniemi RJ. The role of the coil click in TMS assessed with simultaneous EEG. Clin Neurophysiol : official journal of the International Federation of Clinical Neurophysiology 1999;110(8):1325–8.
[70] ter Braack EM, de Vos CC, van Putten MJ. Masking the auditory evoked potential in TMS-EEG: a comparison of various methods. Brain Topogr 2015;28(3):520–8.
[71] Oostenveld R, Fries P, Maris E, Schoffelen J-M. FieldTrip: open source software for advanced analysis of MEG, EEG, and invasive electrophysiological data. Comput Intell Neurosci 2011;2011.
[72] Tadel F, Baillet S, Mosher JC, Pantazis D, Leahy RM. Brainstorm: a user-friendly application for MEG/EEG analysis. Comput Intell Neurosci 2011;2011:879716.
[73] Dale AM, Fischl B, Sereno MI. Cortical surface-based analysis. I. Segmentation and surface reconstruction. Neuroimage 1999;9(2):179–94.
[74] Rogasch NC, Thomson RH, Farzan F, Fitzgibbon BM, Bailey NW, Hernandez-Pavon JC, et al. Removing artefacts from TMS-EEG recordings using independent component analysis: importance for assessing prefrontal and motor cortex network properties. Neuroimage 2014;101:425–39.
[75] Rogasch NC, Biabani M, Mutanen TP. Designing and comparing cleaning pipelines for TMS-EEG data: a theoretical overview and practical example. J Neurosci Methods 2022;371:109494.

[76] Hernandez-Pavon JC, Kugiumtzis D, Zrenner C, Kimiskidis VK, Metsomaa J. Removing artifacts from TMS-evoked EEG: a methods review and a unifying theoretical framework. J Neurosci Methods 2022;376:109591.
[77] Hernandez-Pavon JC, Metsomaa J, Mutanen T, Stenroos M, Maki H, Ilmoniemi RJ, et al. Uncovering neural independent components from highly artifactual TMS-evoked EEG data. J Neurosci Methods 2012;209(1):144–57.
[78] Rogasch NC, Thomson RH, Daskalakis ZJ, Fitzgerald PB. Short-latency artifacts associated with concurrent TMS-EEG. Brain Stimul 2013;6(6):868–76.
[79] Rogasch NC, Sullivan C, Thomson RH, Rose NS, Bailey NW, Fitzgerald PB, et al. Analysing concurrent transcranial magnetic stimulation and electroencephalographic data: a review and introduction to the open-source TESA software. Neuroimage 2017;147:934–51.
[80] Ilmoniemi RJ, Kicic D. Methodology for combined TMS and EEG. Brain Topogr 2010;22(4):233–48.
[81] Mutanen TP, Kukkonen M, Nieminen JO, Stenroos M, Sarvas J, Ilmoniemi RJ. Recovering TMS-evoked EEG responses masked by muscle artifacts. Neuroimage 2016;139:157–66.
[82] Gramfort A, Papadopoulo T, Olivi E, Clerc M. OpenMEEG: opensource software for quasistatic bioelectromagnetics. Biomed Eng Online 2010;9(1):45.
[83] Hyvärinen A, Oja E. Independent component analysis: algorithms and applications. Neural Network 2000;13(4):411–30.
[84] Korhonen RJ, Hernandez-Pavon JC, Metsomaa J, Mäki H, Ilmoniemi RJ, Sarvas J. Removal of large muscle artifacts from transcranial magnetic stimulation-evoked EEG by independent component analysis. Med Biol Eng Comput 2011;49(4):397–407.
[85] Komssi S, Kahkonen S. The novelty value of the combined use of electroencephalography and transcranial magnetic stimulation for neuroscience research. Brain Res Rev 2006;52(1):183–92.
[86] Rogasch NC, Fitzgerald PB. Assessing cortical network properties using TMS-EEG. Hum Brain Mapp 2013;34(7):1652–69.
[87] Komssi S, Aronen HJ, Huttunen J, Kesäniemi M, Soinne L, Nikouline VV, et al. Ipsi- and contralateral EEG reactions to transcranial magnetic stimulation. Clin Neurophysiol 2002;113(2):175–84.
[88] Rajji TK, Sun Y, Zomorrodi-Moghaddam R, Farzan F, Blumberger DM, Mulsant BH, et al. PAS-induced potentiation of cortical-evoked activity in the dorsolateral prefrontal cortex. Neuropsychopharmacology : official publication of the American College of Neuropsychopharmacology 2013;38(12):2545–52.
[89] Brunoni AR, Amadera J, Berbel B, Volz MS, Rizzerio BG, Fregni F. A systematic review on reporting and assessment of adverse effects associated with transcranial direct current stimulation. Int J Neuropsychopharmacol 2011;14(8):1133–45.
[90] Poreisz C, Boros K, Antal A, Paulus W. Safety aspects of transcranial direct current stimulation concerning healthy subjects and patients. Brain Res Bull 2007;72(4–6):208–14.
[91] Miranda PC, Mekonnen A, Salvador R, Ruffini G. The electric field in the cortex during transcranial current stimulation. Neuroimage 2013;70:48–58.
[92] Carbunaru R, Durand DM. Toroidal coil models for transcutaneous magnetic simulation of nerves. IEEE (Inst Electr Electron Eng) Trans Biomed Eng 2001;48(4):434–41.
[93] Deng ZD, Lisanby SH, Peterchev AV. Electric field depth-focality tradeoff in transcranial magnetic stimulation: simulation comparison of 50 coil designs. Brain Stimul 2013;6(1):1–13.
[94] Saturnino GB, Madsen KH, Thielscher A. Electric field simulations for transcranial brain stimulation using FEM: an efficient implementation and error analysis. J Neural Eng 2019;16(6):066032.
[95] Saturnino GB, Puonti O, Nielsen JD, Antonenko D, Madsen KH, Thielscher A. SimNIBS 2.1: a comprehensive pipeline for individualized electric field modelling for transcranial brain stimulation. In: Makarov S, Horner M, Noetscher G, editors. Brain and human body modeling: computational human modeling at EMBC 2018. Cham: Springer International Publishing; 2019. p. 3–25.
[96] Maris E, Oostenveld R. Nonparametric statistical testing of EEG- and MEG-data. J Neurosci Methods 2007;164(1):177–90.
[97] Kahkonen S, Komssi S, Wilenius J, Ilmoniemi RJ. Prefrontal TMS produces smaller EEG responses than motor-cortex TMS: implications for rTMS treatment in depression. Psychopharmacology 2005;181(1):16–20.
[98] Kähkönen S, Wilenius J, Komssi S, Ilmoniemi RJ. Distinct differences in cortical reactivity of motor and prefrontal cortices to magnetic stimulation. Clin Neurophysiol 2004;115(3):583–8.
[99] Komssi S, Kähkönen S, Ilmoniemi RJ. The effect of stimulus intensity on brain responses evoked by transcranial magnetic stimulation. Hum Brain Mapp 2004;21(3):154–64.
[100] Darmani G, Ziemann U. Pharmacophysiology of TMS-evoked EEG potentials: a mini-review. Brain Stimul 2019;12(3):829–31.
[101] Ilmoniemi RJ, Virtanen J, Ruohonen J, Karhu J, Aronen HJ, Näätänen R, et al. Neuronal responses to magnetic stimulation reveal cortical reactivity and connectivity. Neuroreport 1997;8(16):3537–40.
[102] Nitsche MA, Liebetanz D, Schlitterlau A, Henschke U, Fricke K, Frommann K, et al. GABAergic modulation of DC stimulation-induced motor cortex excitability shifts in humans. Eur J Neurosci 2004;19(10):2720–6.
[103] Ferreri F, Pasqualetti P, Maatta S, Ponzo D, Ferrarelli F, Tononi G, et al. Human brain connectivity during single and paired pulse transcranial magnetic stimulation. Neuroimage 2011;54(1):90–102.
[104] Cash RFH, Noda Y, Zomorrodi R, Radhu N, Farzan F, Rajji TK, et al. Characterization of glutamatergic and GABAA-mediated neurotransmission in motor and dorsolateral prefrontal cortex using paired-pulse TMS–EEG. Neuropsychopharmacology : official publication of the American College of Neuropsychopharmacology 2017;42(2):502–11.
[105] König F, Belardinelli P, Liang C, Desideri D, Müller-Dahlhaus F, Gordon PC, et al. TMS-EEG signatures of glutamatergic neurotransmission in human cortex. bioRxiv 2019:555920.
[106] Stagg CJ, Best JG, Stephenson MC, O'Shea J, Wylezinska M, Kincses ZT, et al. Polarity-sensitive modulation of cortical neurotransmitters by transcranial stimulation. J Neurosci 2009;29(16):5202–6.
[107] Purpura DP, McMurtry JG. Intracellular activities and evoked potential changes during polarization of motor cortex. J Neurophysiol 1965;28(1):166–85.
[108] Sun Y, Dhamne SC, Carretero-Guillén A, Salvador R, Goldenberg MC, Godlewski BR, et al. Drug-responsive inhomogeneous cortical modulation by direct current stimulation. Ann Neurol 2020;88(3):489–502.
[109] Premoli I, Castellanos N, Rivolta D, Belardinelli P, Bajo R, Zipser C, et al. TMS-EEG signatures of GABAergic neurotransmission in the human cortex. J Neurosci 2014;34(16):5603.
[110] Connors BW, Malenka RC, Silva LR. Two inhibitory postsynaptic potentials, and GABAA and GABAB receptor-mediated responses in neocortex of rat and cat. J Physiol 1988;406:443–68.
[111] Nikulin VV, Kicić D, Kähkönen S, Ilmoniemi RJ. Modulation of electroencephalographic responses to transcranial magnetic stimulation: evidence for changes in cortical excitability related to movement. Eur J Neurosci 2003;18(5):1206–12.
[112] Bender S, Basseler K, Sebastian I, Resch F, Kammer T, Oelkers-Ax R, et al. Electroencephalographic response to transcranial magnetic stimulation in children: evidence for giant inhibitory potentials. Ann Neurol 2005;58(1):58–67.
[113] Du X, Choa FS, Summerfelt A, Rowland LM, Chiappelli J, Kochunov P, et al. N100 as a generic cortical electrophysiological marker based on decomposition of TMS-evoked potentials across five anatomic locations. Exp Brain Res 2017;235(1):69–81.
[114] Voineskos AN, Farzan F, Barr MS, Lobaugh NJ, Mulsant BH, Chen R, et al. The role of the corpus callosum in transcranial magnetic stimulation induced interhemispheric signal propagation. Biol Psychiatr 2010;68(9):825–31.
[115] Gordon PC, Desideri D, Belardinelli P, Zrenner C, Ziemann U. Comparison of cortical EEG responses to realistic sham versus real TMS of human motor cortex. Brain Stimul 2018;11(6):1322–30.
[116] Biabani M, Fornito A, Mutanen TP, Morrow J, Rogasch NC. Characterizing and minimizing the contribution of sensory inputs to TMS-evoked potentials. Brain Stimulation 2019;12(6):1537–52.
[117] Kuo MF, Paulus W, Nitsche MA. Boosting focally-induced brain plasticity by dopamine. Cerebr Cortex 2008;18(3):648–51. New York, NY : 1991.
[118] Chung SW, Lewis BP, Rogasch NC, Saeki T, Thomson RH, Hoy KE, et al. Demonstration of short-term plasticity in the dorsolateral prefrontal cortex with theta burst stimulation: a TMS-EEG study. Clin Neurophysiol : official journal of the International Federation of Clinical Neurophysiology 2017;128(7):1117–26.
[119] Polanía R, Paulus W, Antal A, Nitsche MA. Introducing graph theory to track for neuroplastic alterations in the resting human brain: a transcranial direct current stimulation study. Neuroimage 2011;54(3):2287–96.
[120] Cosmo C, Ferreira C, Miranda JG, do Rosário R, Baptista A, Montoya P, et al. Spreading effect of tDCS in individuals with attention-deficit/hyperactivity disorder as shown by functional cortical networks: a randomized, double-blind, sham-controlled trial. Front Psychiatr 2015;6(111).
[121] Keeser D, Meindl T, Bor J, Palm U, Pogarell O, Mulert C, et al. Prefrontal transcranial direct current stimulation changes connectivity of resting-state networks during fMRI. J Neurosci : the official journal of the Society for Neuroscience 2011;31(43):15284–93.
[122] Lang N, Siebner HR, Ward NS, Lee L, Nitsche MA, Paulus W, et al. How does transcranial DC stimulation of the primary motor cortex alter regional neuronal activity in the human brain? Eur J Neurosci 2005;22(2):495–504.
[123] Premoli I, Rivolta D, Espenhahn S, Castellanos N, Belardinelli P, Ziemann U, et al. Characterization of GABAB-receptor mediated neurotransmission in the human cortex by paired-pulse TMS-EEG. Neuroimage 2014;103:152–62.
[124] Zhang Y, Chen Y, Bressler SL, Ding M. Response preparation and inhibition: the role of the cortical sensorimotor beta rhythm. Neuroscience 2008;156(1):238–46.
[125] Buschman TJ, Miller EK. Top-down versus bottom-up control of attention in the prefrontal and posterior parietal cortices. Science 2007;315(5820):1860–2.
[126] Womelsdorf T, Schoffelen JM, Oostenveld R, Singer W, Desimone R, Engel AK, et al. Modulation of neuronal interactions through neuronal synchronization. Science 2007;316(5831):1609–12.
[127] Howard MW, Rizzuto DS, Caplan JB, Madsen JR, Lisman J, Aschenbrenner-Scheibe R, et al. Gamma oscillations correlate with working memory load in humans. Cerebr Cortex 2003;13(12):1369–74. New York, NY : 1991.
[128] Bartos M, Vida I, Jonas P. Synaptic mechanisms of synchronized gamma oscillations in inhibitory interneuron networks. Nat Rev Neurosci 2007;8(1):45–56.

[129] Gaetz W, Edgar JC, Wang DJ, Roberts TP. Relating MEG measured motor cortical oscillations to resting γ-aminobutyric acid (GABA) concentration. Neuroimage 2011;55(2):616–21.
[130] van den Broek SP, Reinders F, Donderwinkel M, Peters MJ. Volume conduction effects in EEG and MEG. Electroencephalogr Clin Neurophysiol 1998;106(6):522–34.
[131] Rusjan PM, Barr MS, Farzan F, Arenovich T, Maller JJ, Fitzgerald PB, et al. Optimal transcranial magnetic stimulation coil placement for targeting the dorsolateral prefrontal cortex using novel magnetic resonance image-guided neuronavigation. Hum Brain Mapp 2010;31(11):1643–52.
[132] Romero Lauro LJ, Rosanova M, Mattavelli G, Convento S, Pisoni A, Opitz A, et al. TDCS increases cortical excitability: direct evidence from TMS-EEG. Cortex 2014;58:99–111.
[133] Jamil A, Batsikadze G, Kuo HI, Labruna L, Hasan A, Paulus W, et al. Systematic evaluation of the impact of stimulation intensity on neuroplastic after-effects induced by transcranial direct current stimulation. J Physiol 2017;595(4):1273–88.
[134] Ghasemian-Shirvan E, Mosayebi-Samani M, Farnad L, Kuo M-F, Meesen RLJ, Nitsche MA. Age-dependent non-linear neuroplastic effects of cathodal tDCS in the elderly population: a titration study. Brain Stimul 2022;15(2):296–305.
[135] Ghasemian-Shirvan E, Farnad L, Mosayebi-Samani M, Verstraelen S, Meesen RLJ, Kuo M-F, et al. Age-related differences of motor cortex plasticity in adults: a transcranial direct current stimulation study. Brain Stimul 2020;13(6):1588–99.